



## Trace metal composition of suspended particulate matter in the water column of the Black Sea

Oğuz Yiğiterhan <sup>a,\*</sup>, James W. Murray <sup>b</sup>, Süleyman Tuğrul <sup>a</sup>

<sup>a</sup> Institute of Marine Sciences, Middle East Technical University, PK: 28, Erdemli, Mersin 33731, Turkey

<sup>b</sup> School of Oceanography, Box 355351, University of Washington, Seattle, WA 98195-5351, USA

### ARTICLE INFO

#### Article history:

Received 14 December 2010

Received in revised form 19 May 2011

Accepted 20 May 2011

Available online 27 May 2011

#### Keywords:

Black Sea  
 Geochemistry  
 Biogeochemistry  
 Biogeochemical cycle  
 Trace metals  
 Trace elements  
 Tracers  
 Particulates  
 Suspended particulate matter  
 Biogenic matter  
 Biogenic material  
 Plankton  
 Planktonic metal concentration  
 Redox reactions  
 Redox metals  
 Redox environments  
 Oxidic  
 Suboxic  
 Anoxic  
 Sulfidic  
 Lithogenic  
 Terrestrial  
 Water column  
 Anoxic basin  
 Sediment  
 Brackish water  
 Rivers  
 Danube  
 Turkish rivers  
 Enrichments  
 Depletions

### ABSTRACT

We analyzed the chemical composition of suspended matter from the Black Sea for a complete suite of elements used as tracers for various sources and processes. Samples of suspended matter were collected at four stations from the Bosphorus to the center of the western gyre during a R/V Bilim cruise in September 2000. Sample depths were from the oxic surface layer, the suboxic zone and the upper part of the anoxic (sulfidic) layer. All samples were analyzed for Al, Ti, V, Cr, Mn, Fe, Co, Cu, Zn, Mo, Ag, Cd, Ba, Pb, U and P using ICP-MS, AAS, and spectrophotometer. The main objective of this study was to determine the processes that influence the distributions of particulate trace metals in the water column under various redox environments. The composition of the particulate matter was influenced by lithogenic input from surrounding rivers, biological production in the surface layer, biogeochemical (e.g. redox) processes and anthropogenic inputs. Almost all elemental concentrations decreased from the coastal to the offshore stations to the center of the western gyre. Metal/Al ratios were compared with the ratios of average crust and Danube and Turkish rivers. Deviations from these lithogenic sources were used to examine the anomalies due to geochemical, biological and anthropogenic processes. In general, the largest metal enrichments relative to crust were observed in the surface samples away from coastal sources. Metal/P ratios were used to compare data for some of the elements with previous data from the open ocean. The Me/P ratios for Cu, Zn, Mo and Ni were much higher than open ocean studies, while the ratios for Cd and Co were comparable. The high Me/P (and Me/Al) for several elements suggest anthropogenic input may contribute to these high surface concentrations. The composition of particulate matter from the suboxic zone showed that some elements were strongly enriched. Enrichments of Mn and Fe in the suboxic zone were observed, as expected. Mn and Fe oxides play an important role in scavenging processes. The redox dependent processes in the suboxic - anoxic interface influence the vertical distribution of U, V, Ni, Co, Cu, Zn, Ba and possibly Mo, Cr. Elements influenced by sulfide formation in the anoxic layer were Fe, Cr, Ni, Co, Mo, and Ag.

© 2011 Elsevier B.V. All rights reserved.

### 1. Introduction

Though anoxic basins constitute only a minor part of ocean area and volume, they are important to study because they represent the reducing end-member of the spectrum of ocean redox environments. The biogeochemical cycles of many trace elements are controlled by redox reactions. These elements are important tracers of redox conditions because of their unique geochemical behavior (i.e.,

\* Corresponding author at: Department of Marine Sciences, University of Connecticut, 1080 Shennecossett Road, Groton, CT 06340, USA. Tel.: +1 860 405 9071; fax: +1 860 405 9153.

E-mail addresses: [oguz.yigiterhan@uconn.edu](mailto:oguz.yigiterhan@uconn.edu) (O. Yiğiterhan), [jmurray@u.washington.edu](mailto:jmurray@u.washington.edu) (J.W. Murray), [tugrul@ims.metu.edu.tr](mailto:tugrul@ims.metu.edu.tr) (S. Tuğrul).

tendency to change valence or precipitate as oxides or sulfides) under different environmental conditions (Calvert and Pedersen, 1993; Crusius et al., 1996; Rue et al., 1997; Morford and Emerson, 1999; Yarincik et al., 2000; Nameroff et al., 2002, 2004). Spatial and temporal differences in sediment concentrations of Cd, Cu, Fe, Mn, Mo, Ni, U, V, and Zn have been linked to changes in oxygen concentrations in bottom water and redox conditions of surface sediments. Typically, ratios of elements to Al are used to assess biogeochemical enrichment or depletion relative to detrital concentrations (Nameroff et al., 2002, 2004; Yiğiterhan and Murray, 2008). Morford and Emerson (1999) and Nameroff et al. (2002) summarized the following relationships between redox sensitive particulate element concentrations and redox conditions in sediments from various continental margins. Under oxic conditions, ratios of Cd, Fe, Re, U, and V to Al are at crustal abundances while ratios of Mn and Mo were enriched. In contrast, under anoxic (sulfidic) conditions Fe and Mn are depleted and Cd, Mo, Re, U, and V are enriched relative to crustal material. Mo is more enriched under anoxic than oxic conditions.

Linking the concentration of redox-sensitive metals in sediments to water column oxygen concentrations can be ambiguous because the composition of sediments also depends on redox conditions in the sediment (Calvert and Pedersen, 1993; Nameroff et al., 2002, 2004). For example, enrichments of Cd and U have been observed in anoxic sediments with an overlying anoxic water column (e.g., Black Sea) and in anoxic sediments with an overlying suboxic water column (hemipelagic sediments in the oxygen minimum zone of the eastern tropical Pacific Ocean off Mexico). However, enrichments of Mn and depletions of Cd and U in the sedimentary record are clear indicators that bottom water was not anoxic (Calvert and Pedersen, 1993). Although the behavior of some trace elements in oxic and anoxic environments has been characterized relatively well (Calvert and Petersen, 1993; Piper and Calvert, in press), few studies have been performed on the geochemistry of redox-sensitive trace metals in suboxic geochemical environments. The geochemistry of redox-sensitive elements needs to be better characterized under suboxic conditions if we want to use them for interpreting paleo-sedimentary redox environments.

In the Black Sea there have been a few studies of individual elements but there has been no comprehensive set of analyses of redox sensitive elements in water column particulate matter. In this study, the concentrations of several redox-sensitive elements were measured in suspended particulate matter from the water column in the oxic–suboxic–anoxic layers of the Black Sea. We also analyzed the composition of deep Black Sea sediments, which are solely sulfidic (Yiğiterhan et al., in preparation). A true evaluation of trace elements as proxies should be based on sediments which have undergone the full extent of diagenesis, however the geochemistry of particles in the Black Sea water column is a step in the sequence of reactions. The main objective of this study was to determine the processes that control their distributions and determine whether the suspended particles in the water column have unique geochemical signatures under oxic, suboxic and anoxic (sulfidic) environments.

## 2. Background

### 2.1. The redox environments of the Black Sea

The Black Sea is a semi-enclosed marginal sea with a physical and chemical structure that is determined by its hydrological balance. The salinity increases with depth and this is the main control on the density (Caspers, 1957; Sorokin, 1983). The surface layer (0 to ~75 m) is oxic and the deep water (~125 to 2200 m) is anoxic (sulfidic) (Tuğrul et al., 1992). At the boundary between the oxic and anoxic layers there is a suboxic zone (~50 m thick) where oxygen and sulfide both have very low concentrations and no discernable vertical or horizontal gradients (Murray et al., 1989, 1995). The suboxic zone

varies in thickness at different locations but is often equivalent to a density separation of about  $\Delta\sigma_t = 0.50 \pm 0.10$ . Variability in its thickness is due to variability in physical processes, especially mixing associated with cyclonic and anti-cyclonic eddies (Oğuz et al., 2001a,b; Oğuz, 2002). In the southwest corner of the Black Sea the suboxic zone can be absent due to intrusions from the Bosphorus Plume (Konovalov et al., 2003). Because characteristic chemical and biological features are closely associated with specific density values and these density surfaces dome in the center of the Black Sea, many characteristic features in the vertical profiles occur at different depths but generally fall on the same density surfaces (Vinogradov and Nalbandov, 1990; Codispoti et al., 1991; Lewis and Landing, 1991; Tuğrul et al., 1992; Saydam et al., 1993; Murray et al., 1995). Thus, we use density, rather than depth, as the vertical scale so that we can compare our results from different locations and times. The vertical profiles of oxygen and sulfide for the four stations sampled in this study are plotted versus depth and density in Fig. 1a, b.

The depth of the upper boundary of the suboxic zone is determined by the balance between oxygen injected due to climate driven ventilation of the thermocline (including the Cold Intermediate Layer or CIL located at about 50 m) and oxygen consumed by oxidation of organic matter (Konovalov and Murray, 2001). The injection of oxygen into the upper part of the sulfide zone by ventilation from the Bosphorus Plume is also an important control for the depth of the onset of sulfide (Konovalov and Murray, 2001; Konovalov et al., 2003). Redox reactions involving species of nitrogen, manganese and sulfur are important in the lower part of the suboxic zone (e.g., the N species at the four stations sampled are shown in Fig. 2a) (Oğuz et al., 2001a,b; Fuchsman et al., 2008).

### 2.2. The redox chemistry of trace elements

There have been several studies of dissolved and total trace metal distributions in the Black Sea. Nevertheless, trace metal data for suspended particulate matter are still rare. The chemistry of particles that are introduced to the Black Sea from the atmosphere and rivers is modified by biogeochemical reactions in the different variable redox environments. In addition, new particles are produced in situ by biological and redox processes. During the 1969 R/V Atlantis II cruise (Degens and Ross, 1974), water samples were collected and analyzed for dissolved and particulate trace metals by Spencer and Brewer (1971), Spencer et al. (1972) and Brewer and Spencer (1974). They suggested that there were four fundamental controls on the trace element composition of suspended matter in the water column. These were input of detrital particles, concentration by marine organisms in the surface layers, formation of hydrous metal oxides (e.g.  $\text{MnO}_2(\text{s})$ ,  $\text{Fe}(\text{OH})_3(\text{s})$ ) with adsorption of other trace metals at the oxic/anoxic boundary, and precipitation of sulfide phases in the sulfidic deep waters. Using Mn data, they deduced that about 78% of the detrital load from rivers entering the Black Sea was deposited near the mouth of the rivers and 22% was introduced to the Black Sea. Haraldsson and Westerlund (1988, 1991) also conducted an extensive study of several trace metals and found that major fractions of Cd, Cu, Pb, Zn and Fe are associated with particles. Lewis and Landing (1992) used a sequential filtration-ion-exchange scheme to investigate particulate, colloidal and dissolved speciation of Co, Ni, Cu, Zn, Cd and Pb. Co distributions were best explained by scavenging–recycling with Mn oxides across the sulfide interface and coprecipitation with Fe-sulfides in the deep waters. Ni was unaffected by redox processes. The concentrations of Class B metals (Cu, Zn, Cd and Pb) decreased across the sulfide interface, consistent with metal-sulfide precipitation. Many studies have been conducted of the suspended matter concentrations of individual elements. These include U (Anderson et al., 1989b), Mn and Fe (Tebo, 1991; Lewis and Landing, 1991; Tankere et al., 2001), Ba, (Falkner et al., 1993) and Cu and Zn (Muller et al., 2001).

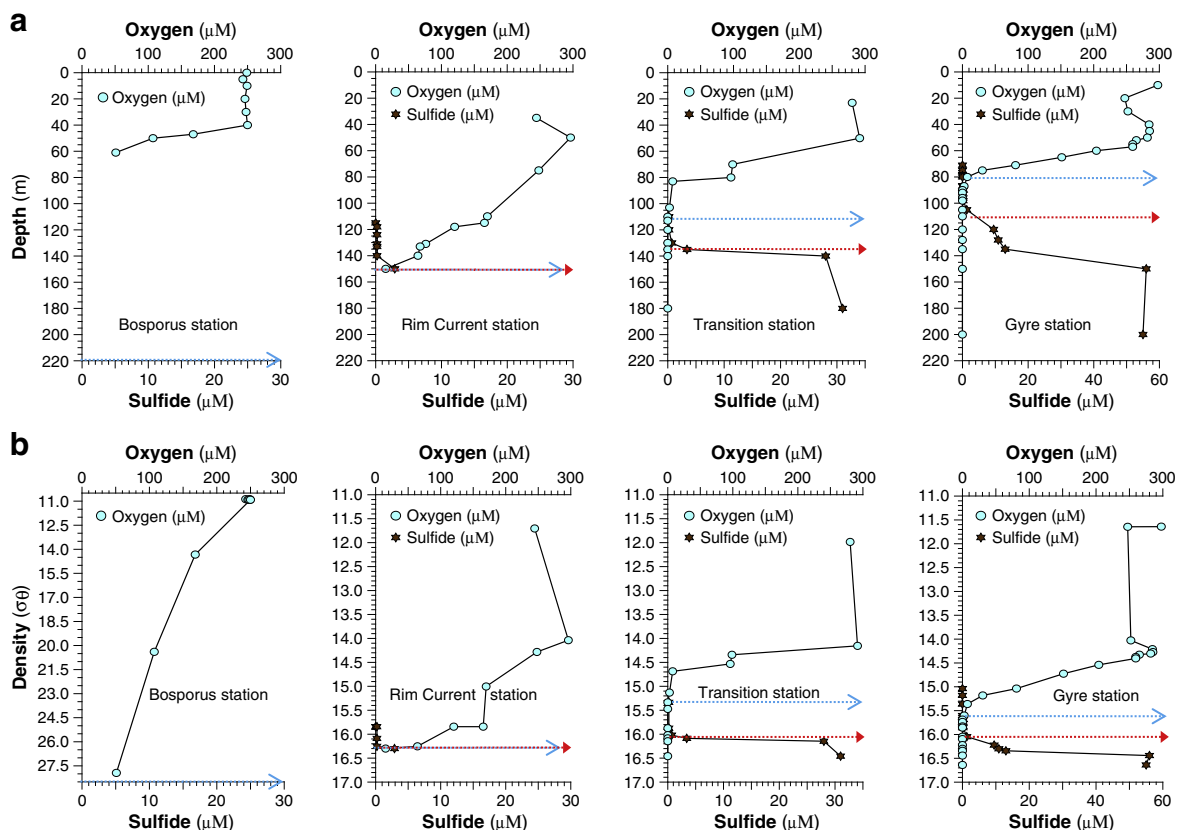


**Fig. 1.** Dissolved oxygen and sulfide concentrations versus depth (a) and density (b) for four Black Sea stations sampled during R/V Bilim September 2000 cruise. The sampling depths and densities are indicated, using shapes and colors: circles for oxygen (ice blue color) and stars for hydrogen sulfide (walnut color) data. The redox layers were shown, using horizontal lines for oxic–suboxic boundary (sky blue colored, open head arrow) and for suboxic–anoxic boundary (red colored, closed head arrow) at their specific depth and densities.

The main goal of this research was to analyze a complete suite of redox sensitive metals on particulate matter samples from the oxic, suboxic and anoxic (sulfidic) zones of the Black Sea. The elements analyzed in this study were Al, Ti, V, Cr, Mn, Fe, Ni, Co, Cu, Zn, Mo, Ag, Cd, Ba, Pb, U and P. Not all of these elements are redox tracers. P is used as a tracer for biological material. Al and Ti are used to estimate the lithogenic fraction of terrestrial origin. Al is one of the key elements in aluminosilicates but has also been shown to be influenced by biological cycling and scavenging. Because Ti (+IV) substitutes for Al (+III) in the lattice of aluminosilicate minerals it is an alternative tracer for lithogenic material. Fe and Mn are redox metals and their cycling is similar. Both form insoluble oxides (Fe + III and Mn + III and +IV) under oxic conditions and both are soluble (Mn + II and Fe + II) under slightly reducing conditions. In the presence of sulfide, Fe(II) forms insoluble FeS(s) and FeS<sub>2</sub>(s) (Emerson et al., 1983). When oxidized, both MnO<sub>2</sub> and FeOOH play an important role as scavenging oxides for other trace metals (e.g., Murray, 1975a,b; Balistrieri and Murray, 1982a,b). Cu and Ba are metals that have been proposed as tracers for planktonic material and analogues for organic carbon export production (Dymond et al., 1992; Paytan et al., 1996; Paytan and Kastner, 1996). Dissolved Ba is generally depleted from surface waters by uptake into particulate matter, derived from biological productivity in surface waters. This association appears due to precipitation of micro BaSO<sub>4</sub> crystals in microzones of decaying biogenic particles (Bishop, 1988). Cd, Ni, Mo are metals used as micro nutrients for plankton growth (Bruland, 1980, 1983; Boyle, 1988), however Cd and Mo as well as Cu, V, Ag, U are also important for their functions in redox reactions. Mo is an essential micronutrient and is utilized in cells in several enzyme systems used for mediating oxygen transfer reactions (Raven, 1988; Fraustu da Silva and Williams, 1991).

Biological utilization of Mo is coupled to both the marine nitrogen cycle and biological Fe-utilization via the enzymes required for nitrogen fixation and nitrate reduction (Stiefel, 1996). Cu shows nutrient-like properties and high concentrations in oxic seawater, but is also influenced by scavenging processes in the ocean water column (Boyle et al., 1977). The speciation of Cu in seawater is dominated by Cu(II) species but it also forms strong complexes with organic matter and has a strong biological affinity. The elements V, Cr, Mn, Fe, Cu, Pb and U have multiple oxidation states whereas Ni, Co, Zn, Mo, Ag, and Cd have only one main oxidation state but they are sensitive to changes in sulfide concentrations (Calvert and Pedersen, 1993, 2007; Nameroff et al., 2002).

### 3. Samples and methods

#### 3.1. Samples

Total suspended matter samples from the water column were collected during the second leg of the R/V Bilim survey cruise, conducted in the southwestern Black Sea between the dates of September 22 to October 1, 2000 by the Institute of Marine Sciences (IMS) of the Middle East Technical University (METU). The stations were located in the Bosporus (Stn. B), shoreward of the Rim Current (Stn. R), at a region between the Rim Current and Western Gyre (Stn. T) and at the center of Western Gyre (Stn. G). The depth and coordinates of these stations are given in Table 1.

Water column samples were collected using acid cleaned 30 L Niskin bottles on a SeaBird CTD rosette. Whole bottle samples were immediately vacuum filtered using acid-cleaned large diameter (142-mm) Nuclepore membrane filters (1.0 μm pore size) mounted in acid

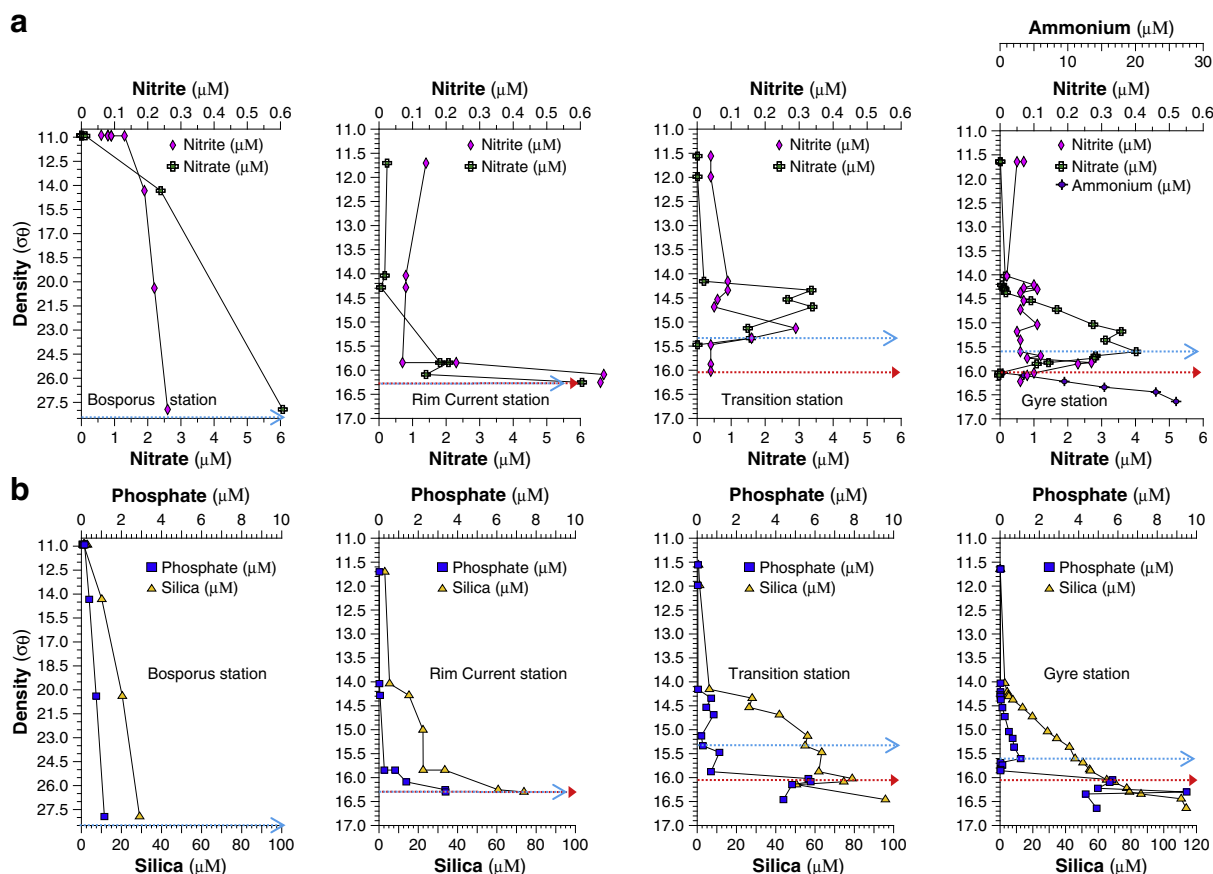


**Fig. 2.** Nitrate and nitrite concentrations versus density (a); phosphate and silica versus density (b) for four Black Sea stations sampled during R/V Bilim September 2000 cruise. The sampling points were indicated using shapes and colors: diamonds (magenta) for nitrite, crosses (grass green) for nitrate, targets (deep river) for ammonia, squares (blue) for phosphate and triangles (deep yellow) for silica data in the plots. The redox layers were shown, using horizontal lines for oxic–suboxic boundary (sky blue colored, open head arrow) and for suboxic–anoxic boundary (red colored, closed head arrow) at their specific densities.

cleaned Plexiglas filter holders. Filtration usually took 1 to 2 h. After a small (0.5–1.0 L) volume is removed quickly for analysis of chemical and nutrient parameters; Niskin bottles were gently mixed just before filtration; then filtration was commenced immediately. During filtration mechanical mixing was repeated for more than four times (in every 15 min) by supporting Niskin bottle horizontally and tilting slowly about 20–30° both directions; and by gently shaking, in order to achieve complete homogenization of suspended particulate matter without unnecessary turbulence; as also recommended later by GEOTRACES intercalibration work. Trace metal clean techniques were applied for all steps in the sampling and filtration process (e.g., Cullen et al., 2001). The filtration was conducted carefully in a semi-closed laboratory of the vessel, through a closed system under low vacuum supplied by Millipore vacuum pumps; without facing any sample contamination problems. Oxygen, sulfide, nutrient, Mn(II), Fe(II), chlorophyll-a and hydrographic data were measured at the same stations and depths as the particulate sampling but sometimes

they were obtained on separate casts. Light transmission and in-situ fluorescence data profiles were also obtained during the rosette casts and were included in the criteria for selection of sampling depths. A unique set of particulate samples was taken from total of 20 different density values, (22 depths) between depths of 10 to 200 m. Filtration volumes varied from 10 to 30 L, with an average of 23.9 L. After filtration the volume of filtrate was measured and the filters were stored frozen in clean plastic bags until acid digestion and analyses were conducted at the University of Washington, School of Oceanography. Unfortunately, the filters were not weighed before and after to get an estimate of total suspended matter mass. However, such weights are often in error due to uncertainty in sea salt and hydration. Our interpretation that follows is based on geochemical approaches, using ratios to Al that we feel are more reliable.

The Nuclepore filters were pre-cleaned by soaking in acid cleaned high-density polyethylene (HDPE) bottles, containing 5% HCl solution and kept at 60 °C for more than 2 days before 10× rinsing with

**Table 1**  
Black Sea sampling stations from the R/V Bilim research cruise in October 2000 where water column samples were collected for total particulate matter. These stations were part of a regular grid of stations sampled by the Middle East Technical University (METU), Institute of Marine Sciences (IMS). The METU-IMS station name, identification and coordinates are also given.

Station description	Station name	R/V Bilim Stn. ID	Latitude	Longitude
Near the Black Sea exit of Bosporus Strait between Rumeli and Anadolu Light Houses, Depth = ~70 m	Bosporus (B)	B-14	41° 11' 68"	29° 05' 96"
In the Rim Current, Depth = ~900 m	Rim Current (R)	L 27–L 18	41° 27'	29° 18'
Between the Rim Current and Western Gyre, Depth = ~1800 m	Transition (T)	L 50–L 20	41° 50'	29° 20'
Center of the Western Gyre, Depth = ~2100 m	Gyre (G)	M 10–L 41	42° 10'	29° 41'

**Table 2**  
The trace element concentrations (ng/cm<sup>2</sup> of filter) for different types of filter material (with their standard deviations and number of filter samples analyzed below). Samples, analyzed for 16 elements, include: a) 142 mm diameter; N.P. = Nuclepore; M.P. = Millipore; Q.M.A. = quartz micro fiber; NITEX = nylon pre-filters; b) 25 mm diameter N.P. and Q.M.A. filters (“A.C.” = Acid cleaned by soaking in diluted hydrochloric acid, “N.C.” = Not pre-cleaned, “L” = Acid leached only, not digested).

Metal	Nuclepore 25 mm, 1.0 μm N.C.	Nuclepore 142 mm, 1.0 μm A.C.	Nuclepore 142 mm, 1.0 μm N.C.	Millipore 142 mm, 1.0 μm A.C.	Supor 142 mm, 0.8 μm A.C.	Q.M.A. 25 mm, 1.0 μm N.C.	Q.M.A. 142 mm, 1.0 μm N.C.	Q.M.A. <sup>L</sup> 142 mm, 1.0 μm N.C.	NITEX 142 mm, 53 μm N.C.
Al	10,420 ± 7930 (13)	620 ± 450 (5)	1990 ± 1190 (3)	3880 ± 5 (5)	1340 ± 540 (6)	1.49E + 07 ± 1.34E + 05 (6)	1.51E + 07 ± 2.20E + 05 (6)	1.03E + 05 ± 1.71E + 04 (5)	12,360 ± 1280 (4)
Ti	<DL (–)	60 ± 51 (7)	<DL (–)	1240 ± 1150 (6)	570 ± 450 (3)	34,660 ± 5420 (6)	46,130 ± 270 (6)	1340 ± 490 (5)	5.56E + 06 ± 3.05 + E05 (6)
V	31 ± 19 (9)	40 ± 28 (9)	19 ± 10 (3)	25 ± 17 (5)	4.5 ± 0.6 (6)	1340 ± 70 (6)	1250 ± 25 (6)	21 ± 5 (3)	150 ± 35 (5)
Cr	7840 ± 2340 (13)	2510 ± 220 (9)	5620 ± 1100 (3)	2840 ± 82 (3)	2950 ± 210 (6)	29,430 ± 2590 (6)	33,950 ± 1540 (6)	<DL (5)	9880 ± 770 (5)
Mn	240 ± NC (7)	35 ± 16 (10)	86 ± 47 (3)	220 ± 5 (3)	3.3 ± 2.9 (5)	18,490 ± 1070 (6)	18,650 ± 85 (9)	1320 ± 410 (5)	23,390 ± 610 (6)
Fe	12,690 ± NC (7)	2290 ± 630 (9)	3630 ± 1540 (3)	2500 ± 1310 (6)	<DL (–)	4.13E + 05 ± 2.62E + 04 (6)	4.28E + 05 ± 5.83E + 03 (6)	50,780 ± 7210 (4)	14,060 ± 3960 (5)
Ni	<DL (–)	731 ± 69 (9)	<DL (–)	101 ± NC (1)	<DL (–)	12,430 ± 900 (6)	13,930 ± 940 (6)	3570 ± 1440 (4)	1900 ± 540 (5)
Co	11 ± 4 (13)	7.5 ± 1.5 (9)	5.9 ± 2.3 (3)	6.1 ± 0.8 (3)	1.2 ± 0.7 (5)	240 ± 1 (6)	260 ± 42 (9)	180 ± 23 (4)	71 ± 26 (5)
Cu	270 ± 320 (13)	310 ± 53 (9)	160 ± 23 (3)	46 ± 4 (3)	9.6 ± 3.9 (6)	2930 ± 220 (6)	2880 ± 180 (6)	1120 ± 840 (5)	3150 ± 430 (5)
Zn	410 ± 50 (11)	850 ± 550 (5)	73 ± 58 (2)	700 ± NC (1)	600 ± 260 (6)	46,240 ± 1810 (6)	48,420 ± 1660 (6)	5140 ± 1280 (5)	37,560 ± 2490 (5)
Mo	100 ± 190 (9)	24 ± 24 (10)	28 ± 10 (3)	16 ± 2 (3)	12 ± 3 (6)	1.72E + 05 ± 2.15E + 03 (6)	1.81E + 05 ± 7.10E + 03 (6)	2650 ± 1190 (5)	127 ± 80 (6)
Ag	34 ± 34 (13)	3.0 ± 2.4 (10)	<DL (–)	2.4 ± 1.2 (6)	<DL (–)	840 ± 33 (6)	720 ± 7 (6)	22 ± 9 (3)	<DL (–)
Cd	<DL (–)	1.5 ± 4.7 (10)	<DL (–)	1.7 ± NC (1)	<DL (–)	200 ± 44 (6)	230 ± 7 (6)	2.6 ± 1.0 (3)	<DL (–)
Ba	330 ± 130 (9)	45 ± 18 (6)	11 ± 12 (3)	260 ± 10 (3)	9.1 ± 2.2 (5)	1.31E + 06 ± 1.77E + 04 (6)	1.32E + 06 ± 3.60E + 03 (3)	70,560 ± 2450 (5)	840 ± 58 (3)
Pb	145 ± 14 (11)	101 ± 7 (9)	53 ± 19 (3)	18 ± 3 (3)	2.6 ± 3.3 (4)	8260 ± 240 (6)	7010 ± 41 (9)	510 ± 190 (5)	150 ± 110 (5)
U	4.2 ± 9.2 (13)	0.7 ± 0.5 (8)	<DL (–)	3.1 ± 2.5 (6)	<DL (–)	3350 ± 35 (6)	3040 ± 10 (9)	77 ± 2 (5)	<DL (–)

**Table 3**  
The depth, hydrographic properties (density, temperature and salinity), water column chemical data (O<sub>2</sub>, H<sub>2</sub>S) and metal concentrations (16 elements) for water column total particulate matter samples, collected from the Bosphorus station (Stn. B), Rim Current station (Stn. R), Transition station (Stn. T), Central Western Gyre station (Stn. G); (D:depth, d: density, T: temperature, S: salinity, <DL: Below detection Limit, – : Not measured).

Bosphorus Stn. (B)																								
Sample #	D (m)	d (σ <sub>θ</sub> )	T (°C)	S (–)	O <sub>2</sub> (μM)	H <sub>2</sub> S (μM)	P (ng/L)	Al (μg/L)	Ti (μg/L)	V (ng/L)	Cr (ng/L)	Mn (μg/L)	Fe (μg/L)	Ni (ng/L)	Co (ng/L)	Cu (ng/L)	Zn (ng/L)	Mo (ng/L)	Ag (ng/L)	Cd (ng/L)	Ba (μg/L)	Pb (ng/L)	U (ng/L)	
1	0	10.914	22.067	17.440	249.2	–	4630	465	21.1	730	830	2.06	168	820	81	259	800	11	3.3	1.9	2.18	190	15	
2	10	10.914	22.067	17.440	249.2	–	5560	520	23.2	830	880	2.47	191	910	98	322	910	11	4.5	3.1	2.22	270	17	
3	20	10.915	22.055	17.437	246.1	–	4330	383	16.8	630	660	1.68	134	810	71	238	680	6.8	2.2	1.5	1.67	170	13	
4	30	10.913	22.067	17.438	247.7	–	5370	502	24.0	870	1470	3.27	193	4340	110	303	790	46	4.7	2.2	1.93	180	17	
5	40	10.914	22.070	17.440	249.9	–	4890	371	20.5	710	800	1.95	151	1080	81	250	610	13	3.5	2.0	1.59	150	14	
Rim Current Stn. (R)																								
Sample #	D (m)	d (σ <sub>θ</sub> )	T (°C)	S (–)	O <sub>2</sub> (μM)	H <sub>2</sub> S (μM)	P (ng/L)	Al (μg/L)	Ti (ng/L)	V (ng/L)	Cr (ng/L)	Mn (μg/L)	Fe (μg/L)	Ni (ng/L)	Co (ng/L)	Cu (ng/L)	Zn (ng/L)	Mo (ng/L)	Ag (pg/L)	Cd (pg/L)	Ba (ng/L)	Pb (ng/L)	U (pg/L)	
6	20	11.11	20.72	17.25	–	–	1620	2.79	180	10	65	0.13	1.94	19	2.2	26	130	3.7	160	1370	1330	21	250	
7	35	11.70	19.02	17.51	245	–	1620	2.61	160	6.1	68	0.09	1.72	9.7	1.2	12	68	3.3	220	1120	990	18	160	
8	50	14.04	8.19	18.13	296	–	210	1.26	73	2.8	70	0.15	0.83	5.6	1.7	7.5	20	0.9	1250	100	42	22	29	
9	75	14.28	7.45	18.34	248	–	350	8.31	420	32	67	0.99	9.42	13	4.5	16	76	0.6	160	410	75	46	300	
10	115	15.84	8.37	20.47	165	<DL	560	18.7	1070	37	170	2.34	11.4	160	8.2	290	160	3.5	890	400	220	95	600	
11	118	15.84	8.37	20.47	120	0.2	380	10.4	710	56	150	32.9	9.15	78	37	180	170	13	570	600	150	99	490	
12	124	16.09	8.52	20.99	67.1	<DL	750	2.94	220	94	46	105	4.09	61	100	46	100	26	300	870	200	22	320	
13	150	16.35	8.55	21.02	15.3	2.9	1880	1.91	120	130	110	144	7.78	52	111	52	160	34	290	680	340	350	380	
14	200	16.62	8.60	21.36	<DL	15.0	290	1.24	70	4.6	57	0.05	1.07	11	3.2	31	63	7.7	280	910	30	14	74	
Transition Stn. (T)																								
Sample #	D (m)	d (σ <sub>θ</sub> )	T (°C)	S (–)	O <sub>2</sub> (μM)	H <sub>2</sub> S (μM)	P (ng/L)	Al (ng/L)	Ti (ng/L)	V (ng/L)	Cr (ng/L)	Mn (ng/L)	Fe (ng/L)	Ni (ng/L)	Co (ng/L)	Cu (ng/L)	Zn (ng/L)	Mo (ng/L)	Ag (pg/L)	Cd (pg/L)	Ba (ng/L)	Pb (ng/L)	U (pg/L)	
15	10	11.56	19.34	17.42	–	–	1680	280	15	7.1	40	69	270	13	0.6	15	31	4.7	210	1250	790	11	100	
16	23	11.99	18.87	17.84	280	–	1410	500	38	6.6	81	78	560	27	0.7	27	23	2.4	370	1020	890	11	60	
17	50	14.16	7.65	18.21	292	–	290	390	110	1.3	42	160	450	6.2	1.0	11	1.7	0.3	160	200	22	6.0	35	
18	80	14.53	7.61	18.68	96.1	–	250	330	5.5	2.0	46	350	410	7.4	1.7	8.2	14	0.7	88	270	54	9.7	16	
19	110	15.34	8.08	19.77	<DL	–	610	200	0.4	11	61	7600	1550	8.6	9.5	9.7	16	2.9	67	170	52	8.5	30	
20	120	15.88	8.38	20.51	<DL	0.2	1550	230	17	4.1	59	720	670	5.0	1.6	83	30	1.5	190	1640	260	8.0	36	
21	130	16.02	8.48	20.71	<DL	0.7	250	440	24	3.8	60	46	410	6.9	1.5	42	85	8.4	125	1870	50	13	48	
22	140	16.15	8.54	20.88	<DL	28.0	270	580	35	3.8	54	190	640	5.1	1.0	56	36	4.3	180	3650	170	17	55	
23	180	16.46	8.55	21.28	<DL	31.0	290	450	34	4.1	50	16	420	7.1	3.3	46	120	8.1	130	1000	28	19	54	
Gyre Stn. (G)																								
Sample #	D (m)	d (σ <sub>θ</sub> )	T (°C)	S (–)	O <sub>2</sub> (μM)	H <sub>2</sub> S (μM)	P (ng/L)	Al (ng/L)	Ti (ng/L)	V (ng/L)	Cr (ng/L)	Mn (ng/L)	Fe (ng/L)	Ni (ng/L)	Co (ng/L)	Cu (ng/L)	Zn (ng/L)	Mo (ng/L)	Ag (pg/L)	Cd (pg/L)	Ba (ng/L)	Pb (ng/L)	U (pg/L)	
24	10	11.64	19.94	17.71	298	–	1610	400	26.7	2.5	130	43	560	35	1.4	15	38	13	120	1000	1480	18	64	
25	30	14.03	8.95	18.23	252	–	680	94	11.5	0.3	75	130	320	7.7	1.5	13	12	0.8	180	180	24	52	10	
26	50	14.30	7.42	18.36	282	–	300	100	10.8	1.6	560	300	1780	660	3.9	11	29	67	17	160	46	7.1	13	
27	80	15.36	7.89	19.78	7.40	<DL	140	85	0.34	0.5	49	330	160	4.2	0.8	6.3	440	0.7	42	130	18	6.8	55	
28	90	15.69	8.00	20.21	<DL	0.3	2150	39	4.71	1.3	46	1130	320	6.1	1.8	6.5	20	1.1	–	120	38	13	35	
29	98	15.86	8.09	20.44	<DL	0.2	790	86	8.96	3.1	48	2710	440	8.3	3.8	13	28	1.8	64	99	53	5.3	47	
30	110	16.04	8.21	20.69	<DL	0.8	610	220	16	2.74	46	310	400	5.6	0.8	58	11	2.1	190	3090	150	7.4	44	
31	120	16.22	8.36	20.95	<DL	9.5	300	330	16	4.69	65	25	360	12	1.5	38	92	7.1	97	1960	67	17	72	
32	135	16.34	8.45	21.12	<DL	13	260	310	15	3.42	44	25	230	6.3	2.0	29	93	6.9	29	1420	23	12	51	
33	150	16.44	8.53	21.26	<DL	56	320	360	20	3.22	56	12	300	8.6	2.6	25	87	7.3	34	1080	140	13	49	
34	200	16.64	8.68	21.54	<DL	55	260	430	24	3.62	370	35	1750	260	6.2	25	74	53	120	760	20	15	64	

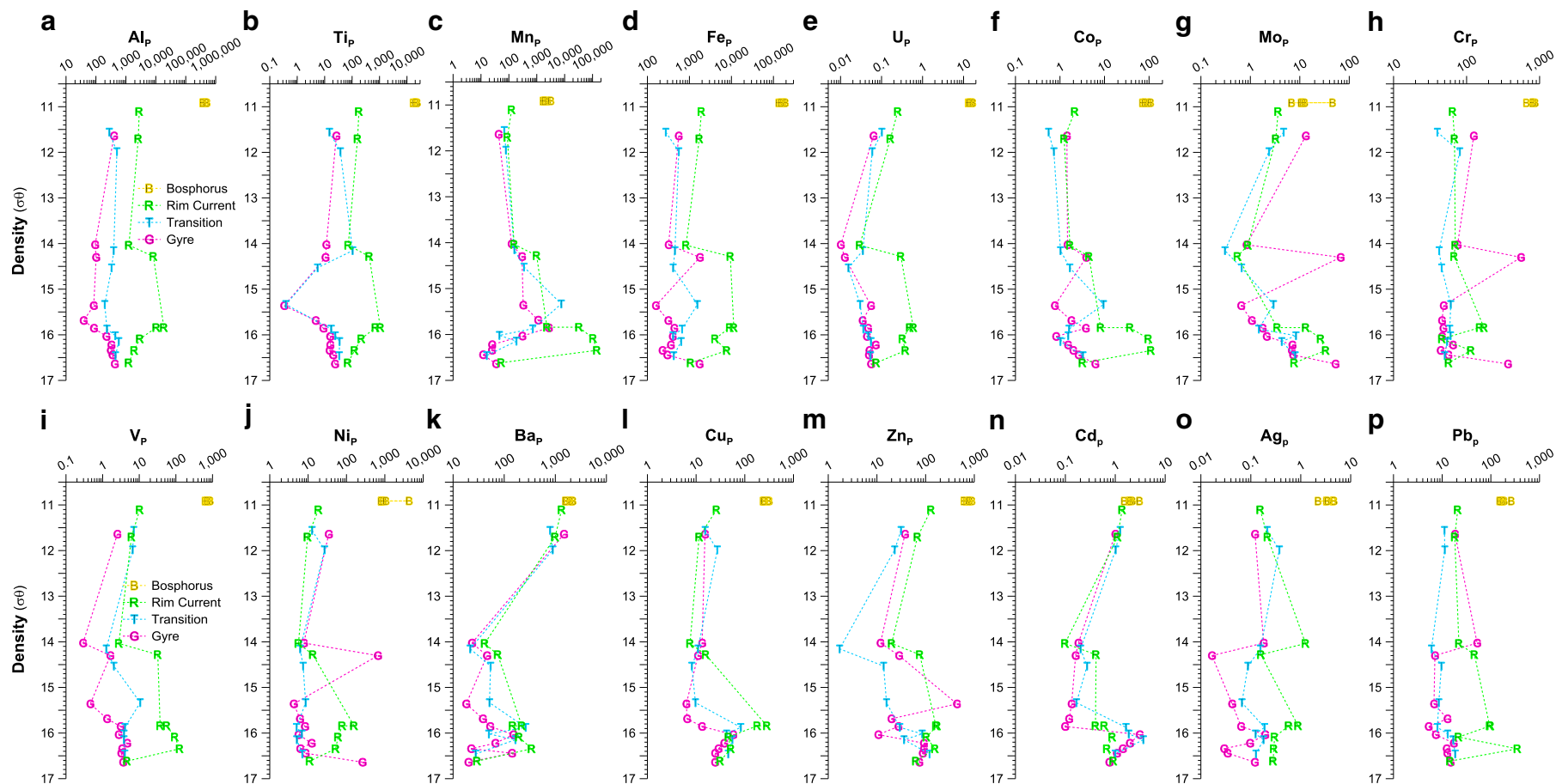


**Fig. 3.** Water column distributions of particulate metal concentrations (ng/L) versus density for 16 elements (a to p) at four Black Sea stations (Bosporus (B), Rim Current (R), Transition (T), and Gyre stations (G)) sampled during R/V Biliim September 2000 cruise. The data was shown on Log scale on X-axis and Linear scale on Y-axis using symbols (initials of stations) and colors: B (yellow), R (green), T (sky blue), G (violet).

deionized water and drying. Filters from the same lot number were kept as filter blanks. Blank filters were always kept separate and handled in the same way as the filters actually used but they were not actually mounted in the filter holder.

### 3.2. Analytical methods

Sixteen redox sensitive metals were analyzed. Analyses were conducted by ICP-MS and GFAAS. Most analyses were done by ICP-MS because it is applicable to a greater number of elements and is faster (Falkner et al., 1995). The isotopes chosen for these analyses were Al<sup>27</sup>,

Ti<sup>48</sup>, V<sup>51</sup>, Cr<sup>52</sup>, Mn<sup>55</sup>, Fe<sup>56</sup>, Ni<sup>58</sup>, Co<sup>59</sup>, Cu<sup>63</sup>, Zn<sup>64</sup>, Mo<sup>98</sup>, Ag<sup>107</sup>, Cd<sup>114</sup>, Ba<sup>138</sup>, Pb<sup>208</sup>, and U<sup>238</sup>. Due to the presence of matrix effects for Ti<sup>48</sup>, we also analyzed Ti<sup>47</sup>. The analytical approach developed for this work utilized microwave digestion of samples. The method of Murray and Leinen (1993), slightly modified by Nameroff (1996), was improved to get more accurate and precise results and used to digest the suspended matter samples. The filters were digested in high pressure Teflon bombs which were acid cleaned (hot-pressurized 30% HNO<sub>3</sub>), rinsed well and dried before starting each new set of digestions.

Thawed, whole filter samples (158.4 cm<sup>2</sup> total surface area) were transferred to 60 mL acid cleaned Teflon bombs (Saville®) using acid

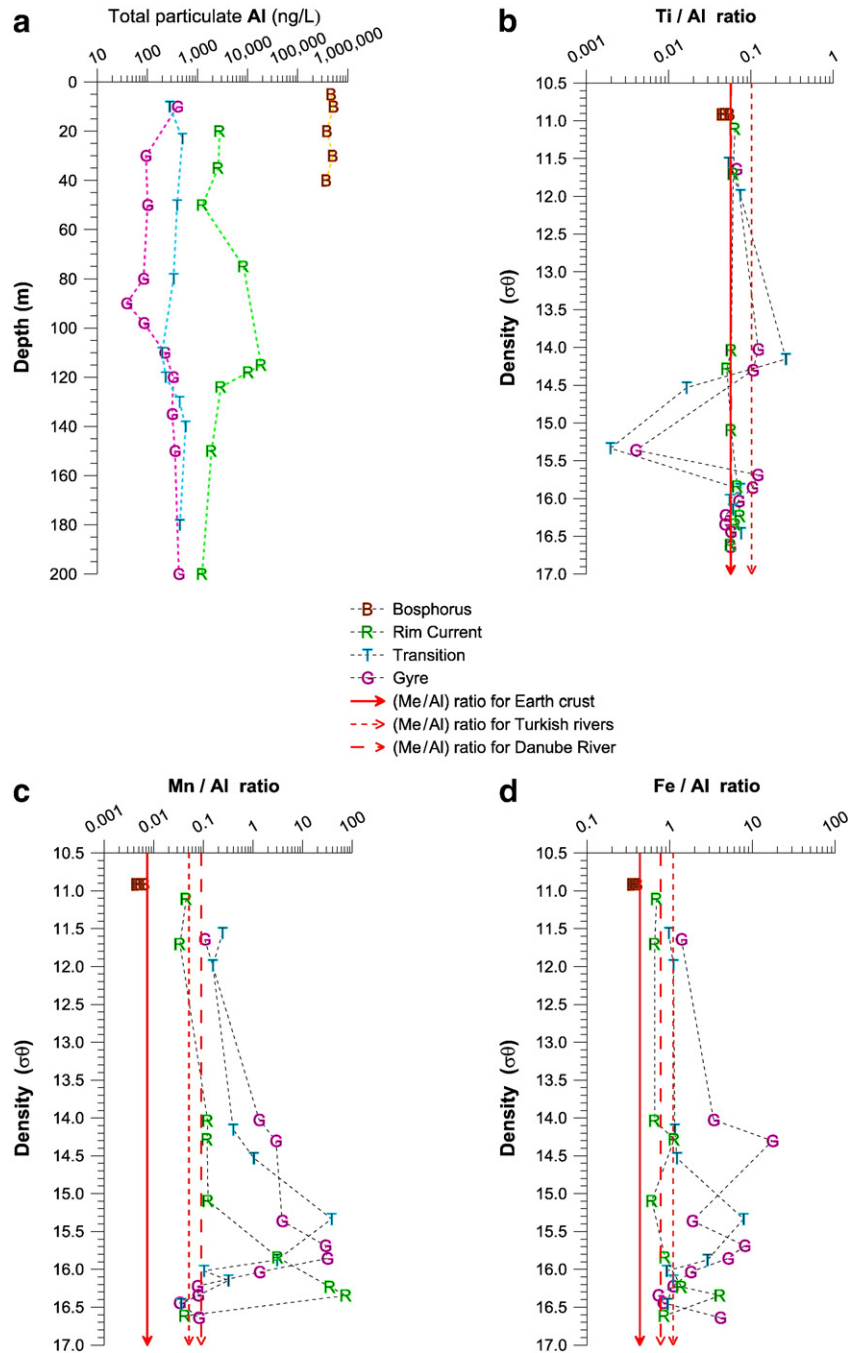


**Fig. 4.** Water column distributions of particulate Aluminum versus depth (a); and metal to Aluminum (Me/Al) ratios versus density for 15 elements together with their comparison with the Me/Al ratios of the average crust, Turkish rivers and Danube River on four Black Sea stations (Bosphorus (B), Rim Current (R), Transition (T), and Gyre (G) stations) were plotted. The data was shown on Log scale on X-axis and Linear scale on Y-axis using symbols (initials of stations) and colors: B (brick red), R (green), T (sky blue), G (hot pink).

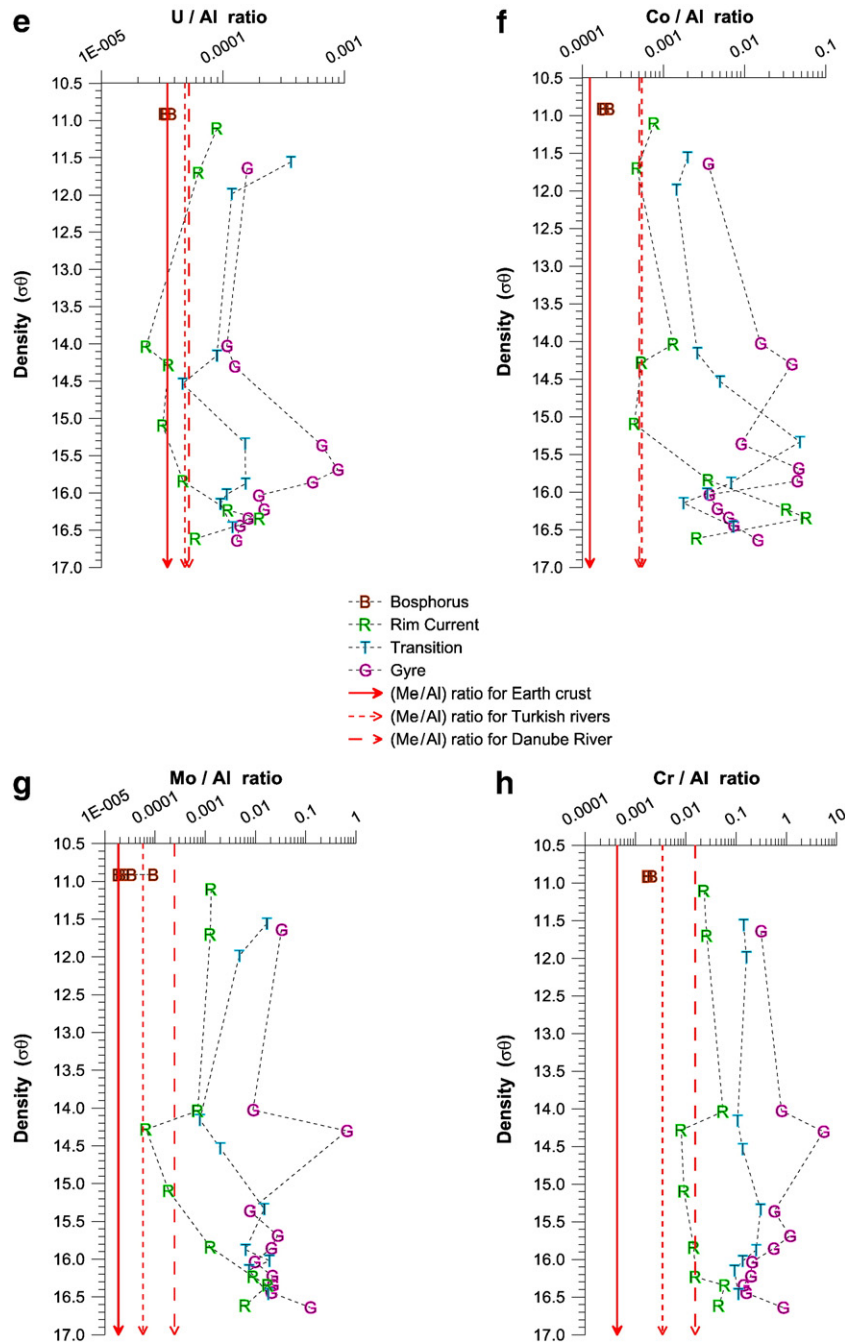


Fig. 4 (continued).

cleaned Teflon tweezers in a dust-free laminar flow fume hood. No samples were punched for sub-samples. Each sample was digested in a cocktail of 4 mL of trace metal grade HF (conc.), 1 mL of each sub-boiling distilled 16 M HNO<sub>3</sub>, and 6 M HCl together with 50 µL of 4 ppm In, Y, Tb as a yield tracer mixture. The acid mixture used was very effective for dissolution of most of the particles. Double distilled deionized water (DDZ) was used for all experimental work. A commercial 1200-Watt microwave was used as a heat source for sample digestion. For the initial digestion, samples were heated for 2 min at 100% and 60 min at 10% power. The acid solutions were transferred to acid-cleaned 50 mL Teflon centrifuge tubes which were placed on a hot plate. These samples were heated to dryness to remove HF and chlorides. An additional 4 mL of HNO<sub>3</sub> was added to the Teflon bombs and filter residue. The bombs were microwaved

another 2 minutes on maximum power followed by 30 min on 10% power. The second digestion solutions were added to the Teflon tubes and dried on the hot plate. Ultrapure reagent grade nitric and hydrogen peroxide (200 µL of HNO<sub>3</sub> and 500 µL of 30% H<sub>2</sub>O<sub>2</sub>) was added at the end of digestion to oxidize any remaining organic matter. The clear, totally dissolved digest was brought to 50 mL final volume and transferred to acid cleaned high-density polyethylene (HDPE) bottles (see Yiğiterhan, 2005 for more details).

The filter digest solutions were analyzed using a Perkin Elmer Sciex ELAN 5000 ICP-MS equipped with AS-90 Autosampler. The ELAN 5000 has a higher sensitivity and lower detection limits than GFAAS for most elements. A Perkin Elmer ELAN 5000 AAS or Hitachi Z-9000 AAS were preferentially used for analyses of Al, Ti, Fe, and Ni. Detection limits based on conventional nebulization ICP-MS (1 mL min<sup>-1</sup>)

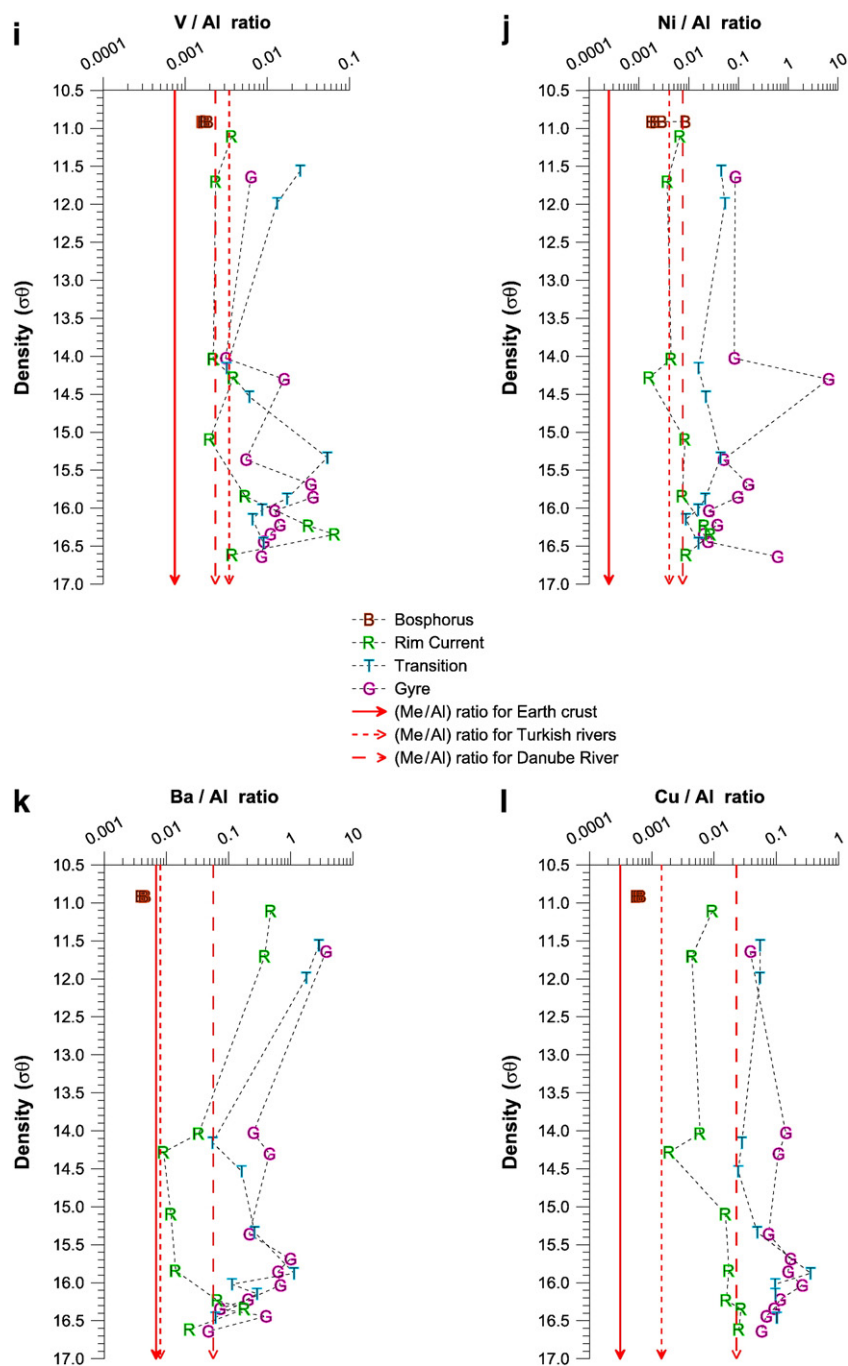


Fig. 4 (continued).

with single ion monitoring are generally on the order of several parts per trillion ( $10^{-12}$ ).

An external standard curve method was used for calculating concentrations. The presence of a large range of concentrations in the particulate matter samples from the oxic surface to the anoxic bottom waters was the main reason we used this approach. The large range of concentrations made other techniques (such as standard additions) difficult to utilize. The mixed standard and internal yield standard solutions were prepared using a background matrix similar to samples. Highly concentrated samples were diluted when necessary to overcome matrix problems and acidified using 1%  $\text{HNO}_3$  in DDZ to provide acidic environment ( $\text{pH}=2$ ) necessary to keep dissolved elements stable in the aqueous sample matrix. We confirmed that

there was no sample matrix problem for the analyzed Nuclepore (NP) filters.

A multi-element standard was prepared in 1%  $\text{HNO}_3$  (v/v) from 1 ppm certified single element standards to obtain concentration ranges typical of surface ocean marine particulate material and was used to calculate the elemental concentrations. Precision was estimated by replicate analyses of actual samples and standard reference materials. Accuracy was determined by analyzing MESS-1 and/or PACS-1 certified sediment reference materials, supplied from National Research Council of Canada. Two different Black Sea sediment samples, collected during R/V Knorr cruises in 1988 and 2001, were used as internal standards for quality control and precision of the analysis. There was always one certified and one Black Sea

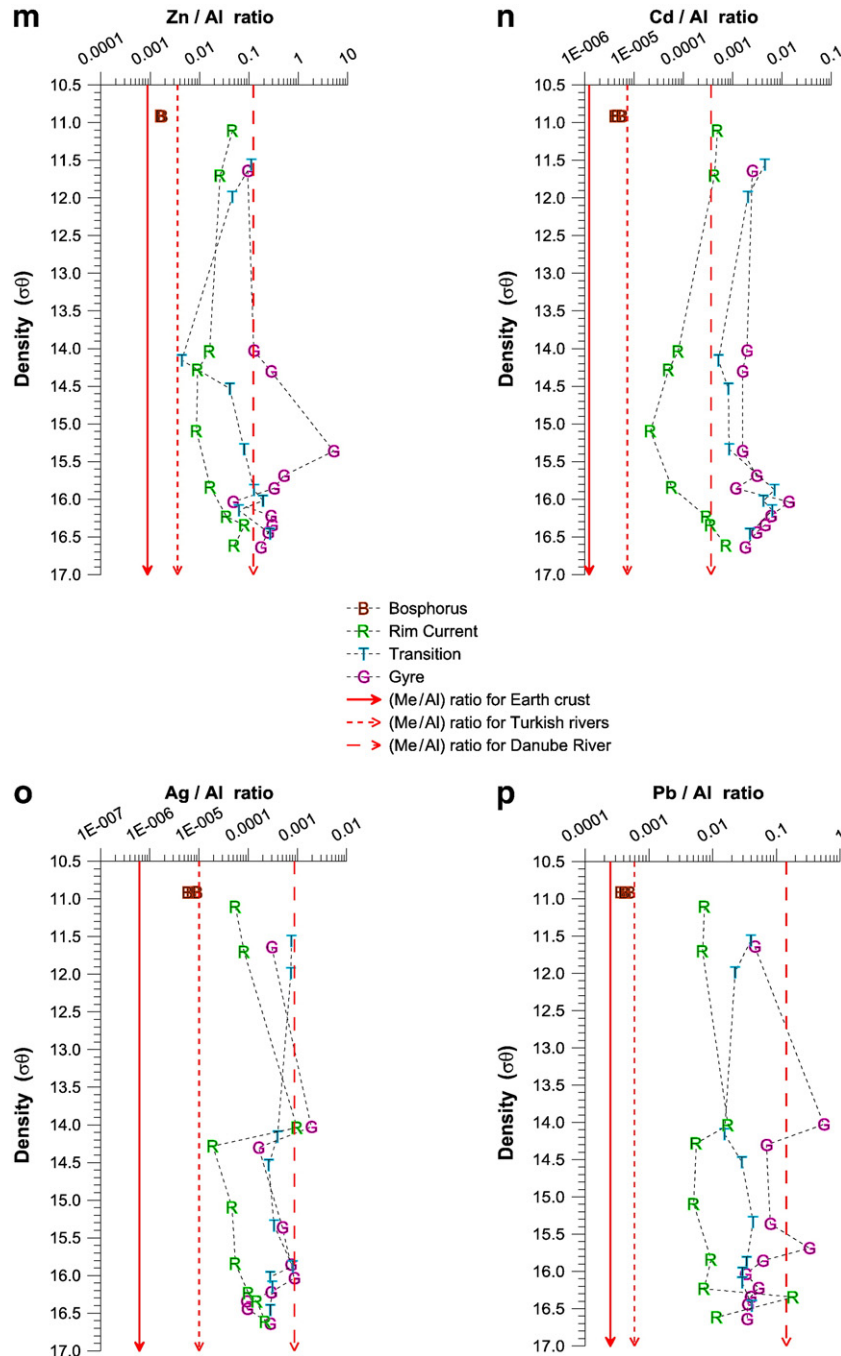


Fig. 4 (continued).

reference standard in each sample set. Yield tracer internal standards were used for volumetric correction of the sample recovered after digestion and helped minimize volumetric errors caused by the evaporation or loss of sample. The mixture was composed of 4 ppm Indium (In), Yttrium (Yt) and Terbium (Tb). These three elements were chosen because of their extremely low natural concentrations in the samples. The final yield tracer concentration of samples was 20 ppb when the digested samples were diluted to 50 mL final volume using 1% HNO<sub>3</sub> (for more details see Yiğiterhan, 2005).

The digested samples were also analyzed for phosphate using an automated version of the ascorbic acid–molybdate method of Murphy and Riley (1962).

### 3.3. Precision and accuracy

Certified reference standard materials (MESS-1 and PACS-1) were analyzed multiple times to calculate precision and to determine the accuracy of analyses and these results were presented in Yiğiterhan and Murray (2008). The precision for most elements was about 5%. However, for Ag and Cd (which have much lower concentrations) the precision was about 10%. In almost all cases the average measured values are within the 95% confidence limits of certified values thus the accuracy determined from this approach was comparable to or better than the precision. The exceptions are Ni where the analyses were higher than the certified value by about 70% and Cr where the

analyses are lower by about 20%. Thus, the analyses in this study were both precise and accurate at acceptable levels.

#### 4. Results

Several filter types are available for filtration of particles from seawater. Selection of the best filter for a specific study involves tradeoffs between the blank values for the filter material and the volume filtration capacity (Cullen et al., 2001). Concentrations of suspended matter were calculated by subtracting the average metal concentration of the blank filters. Thus, determination of accurate values for filter blanks was a crucial step to accurately measure low trace metal concentrations.

We determined the blank values of various types of filters used for sampling suspended matter (Table 2). The purpose was to guide us for the selection of the best type of filter to use for this study. We compared Nuclepore, Millipore, Supor, Q.M.A. (quartz) and Nitex (Nylon) filters. The total blanks varied as different filters were different sizes, thus we calculated the filter blanks on a cm<sup>2</sup> basis (Table 2). Some filters were acid cleaned and others were not. In most cases the filters were totally digested. It was noteworthy that the blanks for the QMA filters were very large for many elements. Thus we also analyzed a QMA filter that was acid leached rather than totally digested. The blank for this case was still large but was much lower than for the totally digested filter.

To determine the blank value for our calculations of particulate trace metals we acid digested ten blank Nuclepore filters (142-mm diameter) (of the type used in this study) in Teflon bombs. Low precision of these filter blank values was a problem but the average blank values were very low and this was more important than their consistency. Three Nuclepore filters (142 mm diameter, 1.0 μm), which were not acid pre-cleaned, were also digested and analyzed in order to evaluate the effect of pre-cleaning on the Nuclepore filters. The acid pre-cleaning resulted in lower and more consistent blank values.

The concentrations of particulate trace metals are presented in Table 3. The depth (m), density ( $\sigma_\theta$ ), temperature (°C), salinity, dissolved oxygen (Winkler), H<sub>2</sub>S and metal concentrations of suspended particulate matter (given in units of μg/L, ng/L or pg/L) are presented in the order of Bosphorus (B), Rim Current (R), Transition (T), and Central Gyre (G) stations. The nutrient data (given in unit of

μM) are presented in the Supplemental Documents. The oxygen and sulfide profiles for our four stations are shown versus depth in Fig. 1.a and versus density in Fig. 1.b. The upper and lower boundaries of the suboxic zone are shown for the Rim Current, Transition and Gyre stations. The first appearance of sulfide is at about the same density at the Transition and Gyre stations but was a little deeper at the Rim Current station. The nitrogen species (nitrate, nitrite and ammonium) are shown versus density in Fig. 2.a. The Transition and Gyre profiles are characterized by a NO<sub>3</sub><sup>-</sup> maximum just above the suboxic zone, NO<sub>2</sub><sup>-</sup> maxima close to the upper and lower boundaries of the NO<sub>3</sub><sup>-</sup> maximum and an increase in NH<sub>4</sub><sup>+</sup> in the anoxic layer (Stn. G only). Silica and phosphorus are shown versus density in Fig. 2.b. Silica mostly increases with depth while PO<sub>4</sub><sup>3-</sup> (especially Stn. G) has the characteristic sequence of a maximum (due to organic matter remineralization), minimum (due to MnO<sub>x</sub> scavenging) and maximum (reduction of sinking MnO<sub>x</sub>, releasing PO<sub>4</sub><sup>3-</sup>) (Shaffer, 1986).

The profiles of particulate trace metals versus density for all four stations are shown in Fig. 3.a to p. The data from the Bosphorus, Rim Current, Transition and Gyre stations are labeled as B, R, T and G, respectively. For Al we show the concentrations versus depth in Fig. 4.a and the metal/Al ratios versus density in Fig. 4.b to p. Depth was used for Al in Fig. 4.a so that the Me/Al ratio plots versus density could be referenced to a depth scale. A log scale is used for the concentrations and Me/Al ratios because the range of values is so large.

Almost all elements had much higher concentrations at the Bosphorus station (Stn. B). The Rim Current station (Stn. R) had systematically higher concentrations than the Transition (Stn. T) and Gyre (Stn. G) stations for Al, Ti, V, Fe, Pb, and U. Mn tended to have higher values in the suboxic zone from  $\sigma_\theta = 15$  to  $\sigma_\theta = 16$  and then decreased to lower concentrations for  $\sigma_\theta > 16$ . In general the composition in the near surface waters ( $\sigma_\theta = 11$  to 12) at all four stations tended to be similar. Some elements (Cu, Ni, Co, Zn, Mo, and Cd) increased with density at density values greater than 16 (in the sulfide zone).

Particulate phosphorus was analyzed as a tracer for organic matter (Cullen et al., 1999). The vertical profiles of particulate P versus density are shown in Fig. 5. Surface layer concentrations were uniformly high: 1620–1676–1613 ng/L (average 1636 ng/L) at Stns. R, T and G. The concentrations at all stations decreased to a minimum at  $\sigma_\theta \approx 14.5$  and then increased to maxima in the suboxic zone. The

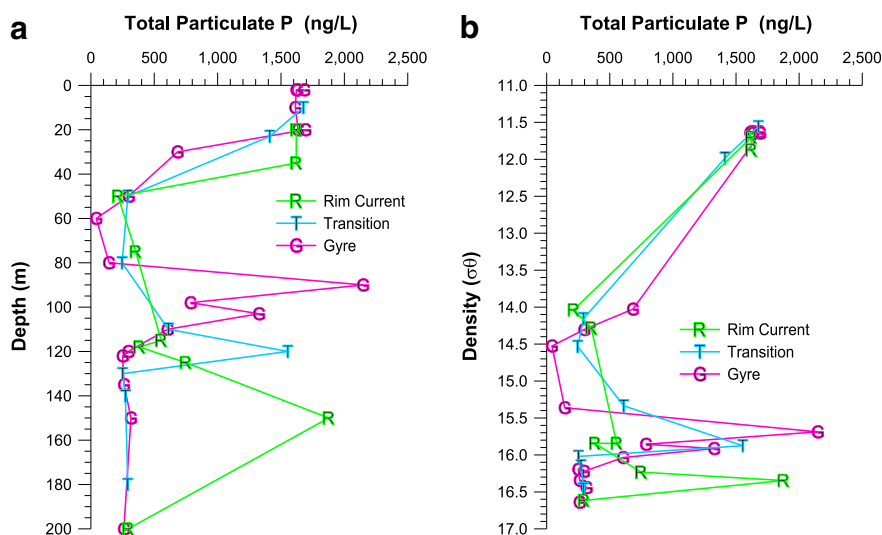


Fig. 5. Particulate phosphorus (P) versus depth (a) and density (b) sampled at three Black Sea stations (Rim Current (R), Transition (T), and Gyre (G) stations) during R/V Bilim September 2000 cruise. The data was shown using symbols (initials of stations) and colors: R (green), T (sky blue), G (hot pink).

concentrations at the Bosphorus station were extremely high and averaged 4957 ng/L (not shown). The origin is not clear but there are many sources of anthropogenic P along the Bosphorus (e.g., Okus et al., 2002).

The concentration anomalies due to biogeochemical processes are superimposed on top of the detrital component. Our approach was to assume that all excess metal over the lithogenic contribution was due to biogeochemical processes. The excess metal concentrations (Me<sub>XS</sub>) were calculated by subtracting the lithogenic material from the measured total particulate metal concentrations. We assumed that Al is a tracer for lithogenic material. This was formulated as:

$$Me_{XS} = Me_{Total} - Me_{Lithogenic}$$

$$Me_{XS} = Me_{Total} - [(Me/Al)_{Rivers} \times Al_{Total}]$$

(Me/Al)<sub>Rivers</sub> were the ratios for average of Turkish Rivers from Yiğiterhan and Murray (2008).

To help understand the relationships between different elements (including phosphorus), and which elements might be controlled by similar processes, we calculated the linear correlations between these excess metal concentrations at various confidence limits (for confidence intervals 90%, 95%, 99%, and 99.9%) using the Excel data analysis tool. The matrix of correlation coefficients is given in Table 4. This shows both positive and negative linear correlations (at P = 0.100), strong linear correlations (P = 0.050 and 0.010) and very strong linear correlations (P = 0.001) (Bevington and Robinson, 1992). In this matrix, correlation co-efficient values are shown for various levels of significances as indicated in the caption. Italic is used together with underlined values for only Ti<sub>XS</sub> vs. V<sub>XS</sub> where the negative correlation coefficient (−0.798) is very close to given confidence limit lower value (−0.805) for P = 0.100. A high (or low) negative correlation has the same interpretation as a high (or low) positive correlation. A negative correlation indicates that high scores in one variable are associated with low scores in the other variable; such as strong negative correlation of Ti<sub>XS</sub> with Zn<sub>XS</sub> (−0.829), V<sub>XS</sub> (−0.798), and Ba<sub>XS</sub> (−0.668). Very strong correlations were observed at 99.9% confidence intervals between Mn vs. V–Co–U–Fe–

Pb; V vs. Co–U–Pb–Fe; Cr vs. Ni–Mo; Fe vs. Pb–U–Co; Ni vs Mo; Co vs. U–Pb; and Ba vs. U. In the following sections we discuss the possible biogeochemical mechanisms, which play important roles for these correlations.

### 5. Discussion

The particulate matter samples are composed of three main components. There are detrital lithogenic materials supplied from rivers and the atmosphere to the oxic surface layer. There are biological materials produced within the euphotic and suboxic zones. There are authigenic metal enrichments caused by geochemical processes such as metal cycling between dissolved (e.g., Mn<sup>2+</sup>, Fe<sup>2+</sup>) and particulate phases (e.g., MnO<sub>2</sub>, FeOOH) in the suboxic zone; and metal sulfide formation (e.g. FeS, FeS<sub>2</sub>) in the anoxic zone. Finally, there may be materials of anthropogenic origin. The lithogenic material is usually unreactive aluminosilicate material of terrestrial origin. Al is often considered a tracer for this fraction (Calvert and Pedersen, 1993). If the trace metal data are plotted as profiles of the metal to Al ratios, anomalies due to biology or geochemistry can be identified as deviations from this background value. The argument is that, if only lithogenic material was present the data would fall along the Me/Al ratio that corresponded to the local detrital silicate sources.

Earth's crustal material is often used to determine the Me/Al ratios for determining anomalies in geochemical distributions. The logic is that if the continental rocks were weathered, then transported to the ocean and buried in sediments, with no modification, the composition of the sediments would be same as the crust. If there are biogeochemical reactions, the sediment composition will differ from the crust and anomalies can be determined. Therefore, some scientists prefer to use the composition of either average crust or shale as reference material to calculate lithogenic material input. Shale is formed from fine-grained sedimentary rock. But because fine-grained sedimentary rocks are frequently organic rich they may have biogeochemical anomalies of redox origin. The two most recent values for the composition of average crust are Taylor and McLennan (1985,

**Table 4** Linear-correlations coefficients for the excess values of 15 metals and particulate phosphorus were determined at various confidence limits (for confidence intervals 90%; 95%, 99%, and 99.9%) using Excel data analysis tool. Correlation co-efficient values are shown for various levels of significances: a) underlined are significant at P = 0.100, b) a plus highlighted green color are significant at P = 0.050, c) b plus bolded are significant at P = 0.010, d) c plus bordered are significant at P = 0.001 (a plus italic is used for only Ti<sub>XS</sub> vs. V<sub>XS</sub> where the negative correlation coefficient (−0.798) is very close to given confidence limit lower value (−0.805) for P = 0.100). The linear-correlation coefficient “R” vs. the number of observations.

	Mn <sub>XS</sub>	Ti <sub>XS</sub>	V <sub>XS</sub>	Cr <sub>XS</sub>	Fe <sub>XS</sub>	Ni <sub>XS</sub>	Co <sub>XS</sub>	Cu <sub>XS</sub>	Zn <sub>XS</sub>	Mo <sub>XS</sub>	Ag <sub>XS</sub>	Cd <sub>XS</sub>	Ba <sub>XS</sub>	Pb <sub>XS</sub>	U <sub>XS</sub>	P
Mn <sub>XS</sub>	1.000															
Ti <sub>XS</sub>	<u>−0.388</u>	1.000														
V <sub>XS</sub>	<b>0.997</b>	<u>−0.798</u>	1.000													
Cr <sub>XS</sub>	<u>−0.047</u>	<u>−0.285</u>	<u>−0.043</u>	1.000												
Fe <sub>XS</sub>	<b>0.787</b>	<u>−0.418</u>	<b>0.798</b>	0.271	1.000											
Ni <sub>XS</sub>	<u>−0.030</u>	<u>−0.262</u>	<u>−0.027</u>	<b>0.968</b>	0.232	1.000										
Co <sub>XS</sub>	<b>0.995</b>	<u>−0.623</u>	<b>0.987</b>	<u>−0.009</u>	<b>0.748</b>	0.018	1.000									
Cu <sub>XS</sub>	0.109	<u>−0.072</u>	0.208	0.005	0.276	<u>−0.024</u>	0.279	1.000								
Zn <sub>XS</sub>	0.224	<u>−0.829</u>	0.163	<u>−0.062</u>	0.158	<u>−0.077</u>	0.199	0.118	1.000							
Mo <sub>XS</sub>	<u>0.343</u>	<u>−0.272</u>	0.328	<b>0.894</b>	<b>0.531</b>	<b>0.868</b>	<b>0.371</b>	<u>−0.037</u>	0.031	1.000						
Ag <sub>XS</sub>	0.080	0.448	<u>0.399</u>	<u>−0.096</u>	0.207	<u>−0.136</u>	0.119	<b>0.393</b>	<u>−0.116</u>	<u>−0.155</u>	1.000					
Cd <sub>XS</sub>	<u>−0.078</u>	0.639	<u>−0.125</u>	<u>−0.194</u>	<u>−0.062</u>	<u>−0.209</u>	<u>−0.117</u>	0.089	<u>−0.111</u>	<u>−0.116</u>	<u>−0.181</u>	1.000				
Ba <sub>XS</sub>	0.029	<u>−0.668</u>	<u>−0.007</u>	<u>−0.071</u>	<u>−0.040</u>	<u>−0.105</u>	<u>−0.030</u>	<u>−0.133</u>	<u>−0.068</u>	<u>−0.077</u>	<u>−0.045</u>	0.175	1.000			
Pb <sub>XS</sub>	<b>0.778</b>	<u>−0.278</u>	<b>0.816</b>	0.031	<b>0.908</b>	<u>−0.018</u>	<b>0.752</b>	0.285	0.204	0.246	0.182	<u>−0.124</u>	<u>−0.002</u>	1.000		
U <sub>XS</sub>	<b>0.954</b>	<u>−0.186</u>	<b>0.926</b>	<u>−0.116</u>	<b>0.792</b>	<u>−0.103</u>	<b>0.897</b>	0.223	0.282	0.244	<b>0.376</b>	<u>−0.043</u>	0.210	<b>0.797</b>	1.000	
P	0.308	<u>−0.403</u>	0.298	<u>−0.144</u>	0.303	<u>−0.156</u>	0.246	<u>−0.079</u>	<u>−0.161</u>	<u>−0.080</u>	<u>−0.015</u>	<u>−0.009</u>	<b>0.677</b>	0.293	<b>0.417</b>	1.000
For N values →	24	5	24	29	16	27	26	29	29	29	28	29	29	29	24	29
P ↓ values	R ↓ values															
if, P = 0.100 →	R =	0.344	0.805	0.344	0.311	0.426	0.323	0.330	0.311	0.311	0.317	0.311	0.311	0.311	0.344	0.311
if, P = 0.050 →	R =	0.404	0.878	0.404	0.367	0.497	0.380	0.388	0.367	0.367	0.374	0.367	0.367	0.367	0.404	0.367
if, P = 0.010 →	R =	0.515	0.959	0.515	0.471	0.623	0.487	0.496	0.471	0.471	0.479	0.471	0.471	0.471	0.515	0.471
if, P = 0.001 →	R =	0.629	0.991	0.629	0.579	0.742	0.597	0.607	0.579	0.579	0.579	0.588	0.579	0.579	0.629	0.579

1995) and Wedepohl (1968, 1995). The best approach for a specific study site is to use detrital particles of local origin. Yiğiterhan and Murray (2008) compared the composition of suspended particles and sediments from the Danube River and four Turkish rivers (Sakarya, Yenice, Kızılırmak, and Yeşilirmak) with crust and shale. They recommended that the best choice for the composition of local detrital material of natural origin was the average of the suspended matter from Turkish rivers and the surface sediments from the Danube River. The composition from these sources actually agreed well with estimates of average crust. Suspended particles from the Danube River tend to be enriched in many trace metals, suggesting anthropogenic contamination (Guieu and Martin, 2002).

### 5.1. Metal enrichments and depletions

The total suspended aluminum concentrations and the Me/Al ratios (except for Al) are plotted versus density for 15 elements in Fig. 4. Suspended aluminum is plotted versus depth to display the depth dependence of this reference element. The symbols B, R, T and G are used for the data from the stations sampled. Solid and dashed lines are also drawn to indicate the reference Me/Al ratios of average crust and riverine waters (average of four Turkish rivers and Danube River), respectively. We were not able to distinguish between terrigenous particles from Eastern Europe and the Anatolia/Southern Caucasus as done by Piper and Calvert (in press).

At Station B, Me/Al ratios for most elements were similar to average global crust and slightly less than the average Me/Al ratios for Turkish rivers. These samples were all from the surface (0–40 m) water in the north end of the Bosphorus which is water flowing out of the Black Sea. Thus the composition of these particles should be representative of surface samples in the coastal region of the SW Black Sea. The Me/Al ratios at Stn. R are also uniform but slightly elevated over ratios for Turkish rivers and less than the ratios for the Danube River. The ratios at Stns. T and G show indications for different elements of enrichment in the surface samples, enrichments in the suboxic zone, possibly due to scavenging by metal oxides, and enrichments in the sulfide layer. Based on the profiles of the concentrations and Me/Al ratios the particulate distributions can be described.

The elements will be discussed in the following sequence: detrital tracers (Al, Ti), metal oxide cycling (Mn, Fe), redox sensitive (U, Co, Mo, Cr, V), organic matter flux (Ni, Ba) and class B (Cu, Zn, Cd, Ag, Pb).

#### 5.1.1. Aluminum

Al is usually used as a tracer for terrestrial input of detrital aluminosilicate material (e.g., Calvert and Pederson, 2007). Particulate Al distributions in most coastal ocean environments are dominated by lithogenic material. However, in some sediments there is evidence that Al may be associated with the Mn/Fe oxide fraction (Kryc et al., 2003).

Lewis and Landing (1991) observed that suspended Al profiles (e.g.  $Al_p$ ) in the Black Sea had a maximum in the upper 5–50 m and another broad maximum below the sulfide interface. In our data set, concentrations of  $Al_p$  were high and constant with depth at the Bosphorus station (B) (Fig. 4.a). There were no surface maxima at the other three Black Sea stations (R, T and G) but the concentrations of  $Al_p$  decreased sharply ( $\sim 1000\times$ ) from the Bosphorus to the Transition station then to the Gyre station especially above the suboxic zone. There was a large subsurface maximum of  $Al_p$  at the Rim Current station close to the depth of the shelf break (Fig. 4.a). There was not an equivalent maximum of  $Al_p$  at Stns. T and G. So if sediment resuspension was important it was limited to the region of the Rim Current (Stn. R). The gradient of  $Al_p$  in the surface layer suggests that the origin of  $Al_p$  must be from river runoff and/or resuspended shelf sediments. The inputs from local Turkish rivers (e.g. the Sakarya and Yenice Rivers) are especially large (Yiğiterhan and Murray, 2008).

At the Transition and Gyre stations,  $Al_p$  decreased to a slight minimum in the suboxic zone and then increased into the sulfide zone. Offshore transport of resuspended sediment is the most likely source for these high values in the sulfide zone. The minima in  $Al_p$  at the depth where  $O_2$  decreases to zero may result from scavenging of Al particles from water column by organic matter produced locally (e.g. chemosynthesis) or by removal associated with removal of Mn/Fe oxides.

#### 5.1.2. Titanium

Particulate Ti is very insoluble, with no significant solution chemistry (Orians et al., 1990). It should be an excellent tracer for lithogenic material of terrestrial origin. Titanium is also used as a tracer for heavy minerals that host Ti, like illmenite ( $FeTiO_3$ ) and rutile ( $TiO_2$ ), and thus is sometimes used as a tracer for grain size (e.g., Calvert and Pederson, 2007). But the sources and distributions of Ti in the ocean are not totally understood. For example, Kryc et al. (2003) found that when the detrital flux is low (such as the equatorial Pacific) there are indications of excess Ti associated with an organic matter phase. Skrabal and Terry (2002) observed that Ti is mobilized in the pore water of estuarine and coastal marine sediments and Skrabal (2006) showed that the Ti flux from the sediments can influence water column distributions.

The profiles of particulate Ti and Al (Fig. 3.b and a) were similar at all stations. The Ti/Al ratios in the Black Sea particles are generally very similar to crust and Turkish rivers at all stations with one exception (Fig. 4.b). There is a significant minimum in the Ti/Al ratio at  $\sigma_\theta \approx 15.4$  at the two offshore stations (T and G). This density corresponds to the upper boundary of the suboxic zone. The fact that it was seen at two stations, in several samples and at the same density suggests this feature is not a sampling artifact or due to bad analyses. The total concentration of Ti was also a minimum at that depth. There is no indication from the Al concentration profile that Al is enriched. So this low Ti/Al ratio appears due to low Ti rather than high Al. It appears that Ti has been removed from the particles. This appears to be a valid feature for which we have no certain explanation, except that it indicates an uncoupling of the distributions of Ti and Al at those depths. There must be exceptions to our assumption that Al and Ti are associated only with detrital material and always correlate strongly with each other. This assumption was supported by the strong negative correlation of  $Ti_{XS}$  with  $Zn_{XS}$  ( $-0.829$ ),  $V_{XS}$  ( $-0.798$ ), and  $Ba_{XS}$  ( $-0.668$ ) (Table 4) which are three elements that show nutrient like distributions due to biological cycling.

#### 5.1.3. Manganese

Manganese is one of the main metals which display an active recycling between oxidized and reduced forms across the redox boundaries of the Black Sea (Spencer and Brewer, 1971; Lewis and Landing, 1991; Calvert and Pedersen, 1993; Yemenicioğlu et al., 2006). In oxygenated seawater Mn exists primarily as insoluble Mn(III, IV) oxyhydroxides (e.g.,  $MnO_x$ ) like  $MnOOH(s)$  and  $MnO_2(s)$  (Tebo, 1991). Soluble Mn(III), stabilized by dissolved ligands, is an important intermediate in Mn cycling and can constitute up to 100% of the dissolved Mn pool (Trouwborst et al., 2006). Microbially mediated oxidation plays an important role in the formation of these oxides (e.g., Mandernack et al., 1995; Bargar et al., 2005).  $MnO_x$  particles are important substrates for the scavenging of other trace metals (Murray, 1975a,b; Klinkhammer and Bender, 1980; Bruland, 1983; Burton and Stratham, 1988) and phosphate (Shaffer, 1986). Sinking particulate  $MnO_x$  is reduced to more soluble Mn(II), perhaps by reaction with dissolved sulfide (Konovalov et al., 2003). Solubility calculations suggest that reduced Mn present as  $Mn^{2+}$  can precipitate as MnS (manganese sulfide),  $MnS_2$  (haurite) (Emerson et al., 1983; Lewis and Landing, 1991) or  $MnCO_3$  (rhodochrosite; Spencer and Brewer, 1971; Haraldsson and Westerlund, 1988). Suess (1979) observed formation of  $\gamma$ -MnS (wurtzite) in Baltic Sea sulfide rich

sediments. Solid Mn(III) oxides (e.g.,  $\gamma$ MnOOH) can form as intermediates during the oxidation of Mn(II) (Murray et al., 1985).

The vertical profiles of particulate manganese ( $Mn_p$ ) typically show a maximum in the suboxic zone (Fig. 3.c).  $Mn_p$  concentrations were approximately 20 fold higher in the oxic–anoxic interface of the Rim Current station than at the upper boundary of the suboxic layer at the Transition station. The amount of particulate Mn decreased to 50–60 times lower values in the suboxic layer of the Gyre station. These concentrations are similar to those of Konovalov et al. (2003) who used data from the Knorr 2001 cruise. The Mn enrichments observed at the Rim Current station are possibly due to 1) the large fluxes of Mn(II) from slope sediments in contact with the density surfaces of the suboxic zone (Konovalov et al., 2007) and 2) the lateral influx of  $O_2$  associated with the Bosphorus Plume which could result in oxidation of dissolved  $Mn^{2+}$  to form  $MnO_2$  (Konovalov et al., 2003).

The Mn/Al ratios show that there is excess Mn relative to crustal values at most stations in the Black Sea (Fig. 4.c). The values at Stn. B are constant and very close to average crust. There is excess Mn in the samples at  $\sigma_\theta \geq 14.2$  from the Rim Current. The enrichments close to the southeastern region at the Rim Current station are due to lateral influx of  $O_2$  associated with the Bosphorus Plume, which dramatically affect the redox budget of the system and result in variations in the distribution of the main reduced redox species (Konovalov et al., 2003). There are large amounts of excess Mn at Stns. T and G in the suboxic zone between densities of  $\sigma_\theta = 14$  to 16. Maximum Mn values occur at  $\sigma_\theta = 15.70$ – $15.95$  at the Gyre station and  $\sigma_\theta = 15.35$  at the Transition station. These are the densities showing the upper boundaries of the anoxic layers at Stns. G and T. Mn is enriched relative to average of Turkish rivers by more than 100 fold. We did not measure Mn oxidation states but these large amounts of excess Mn have been shown previously to be present as Mn(IV) oxides, not as scavenged Mn. Based on analyses by XANES, Tebo et al. (2004) concluded that  $\delta MnO_2(s)$  was the most likely solid phase in the Black Sea. Even though  $O_2$  concentrations are low there must be enough to oxidize Mn(II). Particulate P has a maximum at  $\sigma_\theta = 16.0$  which is the same depth as particulate Mn. The most likely hypothesis is that particulate Mn oxides scavenge P. But this requires more focused research.

Excess Mn is strongly correlated with  $Fe_{XS}$ ,  $V_{XS}$ ,  $Co_{XS}$ ,  $Pb_{XS}$  and  $U_{XS}$  (Table 4). The fact that  $Mn_{XS}$  and  $Fe_{XS}$  (and associated scavenged elements) are mutually correlated means that this is a group of elements associated with metal oxide cycling but that our sample resolution was not sufficient to separate Fe cycling from Mn cycling.

#### 5.1.4. Iron

Iron is often enriched as oxidized Fe(III) oxyhydroxides under oxic conditions (Murray, 1979) and is reduced to Fe(II) under reducing conditions. Past work in the Black Sea has shown that oxidative precipitation of Fe does not result in unusually high particulate Fe concentrations above the sulfide interface although measurable Fe enrichment has been observed in the Fe/Al ratios (Lewis and Landing, 1991). The distribution and redox cycling of Fe is similar to Mn but the dissolved concentrations of Fe are lower than for Mn (Murray and Yakushev, 2006). Both Mn(IV) and Fe(III) oxides formed in the suboxic zone may be reduced by reaction with sulfide (e.g., Millero, 1991). Like Mn(II), Fe(II) is more soluble in the reduced oxidation state, but when Fe is reduced in seawater it does not increase to concentrations as high as Mn because Fe(II) tends to precipitate as insoluble FeS minerals (Spencer et al., 1971). Sulfidic waters in the Black Sea have been shown to be close to or above saturation with respect to FeS (mackinawite) or  $Fe_3S_4$  (greigite) (Brewer and Spencer, 1974; Emerson et al., 1983; Lewis and Landing, 1991).

In our data set the highest concentrations of particulate iron were observed at the Bosphorus station (B) where the amount of particulate Fe in surface samples was hundreds of times higher than the other stations (Fig. 3.d). Based on the Fe/Al ratios, there was no excess Fe

at Stn. B and very little, if any, at Stn. R, relative to the crustal background (Fig. 4.d). There are 10 fold or greater anomalies of excess Fe in the suboxic zone at Stns. T and G suggesting enrichment due to formation of iron oxides resulting from redox cycling (Yemenicioğlu et al., 2006). Maximum enrichments at Stn. T are at  $\sigma_\theta = 15.3$  and at Stn. G at  $\sigma_\theta = 14.3$  and  $\sigma_\theta = 15.7$ . These are the same densities where the maximum Mn/Al ratios were found. The Fe/Al ratio increased in the sulfide layer at Stn. G, probably due to formation of particulate iron sulfides. Muramoto et al. (1991) observed well formed pyrite framboids in sediment trap samples and proposed that pyrite formation was active in the upper layer of the sulfidic zone. Excess Fe is significantly correlated with  $Mn_{XS}$ ,  $V_{XS}$ ,  $Co_{XS}$ ,  $Mo_{XS}$ ,  $Pb_{XS}$ , and  $U_{XS}$  (Table 4).

#### 5.1.5. Uranium

Uranium concentrations are conservative in oxygenated seawater, because oxidized U(VI), forms stable, soluble, anionic complexes with carbonate ion (Langmuir, 1978). Since thermodynamics predict that U(VI) can be reduced to insoluble U(IV) at about the same redox potential as  $SO_4^{2-}$  reduction, the early predictions were that U would be reduced and enriched in particles in the deep sulfidic waters of the Black Sea (Anderson et al., 1989). Contrary to this expectation, dissolved U(VI) was found to be neither reduced to the thermodynamically favored U(IV) nor was it scavenged from the water column by particles (Anderson et al., 1991). Kinetic factors must play an important role.

The U/Al ratios at Stn. B were exactly the same as the crustal value (Fig. 4.e). There were elevated concentrations of U in the surface samples at Stns. R, T and G (Fig. 3.e) and this might be due to biological enrichment since the U/Al ratios were enriched as well. Particulate U concentrations ( $U_p$ ) increased in the suboxic layer in a manner similar to particulate P, which suggests there may be similar particulate enrichment processes for both P and U (Figs. 5 and 4.e).

The U/Al ratios at Stn. R were similar to the crustal ratios except for samples from the sulfide layer. There was excess Fe in the same samples probably due to iron sulfide formation. The uranium enrichment may be due to scavenging of U by iron sulfide particles. There was also excess U in the suboxic zone at Stns. T and G. The similarities of excess  $U_p$  and excess  $Mn_p$  at  $\sigma_\theta = 15.6$  are strong at these two stations so these enrichments may be due to scavenging of U by Mn/Fe oxyhydroxides, even though U is thought to be conservative.  $U_{XS}$  and  $Mn_{XS}$  are strongly correlated ( $r^2 = 0.95$ , Table 4) which supports this scavenging hypothesis.

#### 5.1.6. Cobalt

Cobalt is in the Co(II) oxidation state in seawater, primarily as the  $Co^{2+}$  ion which forms chloro- and carbonato-complexes (Bruland, 1983). There is no evidence that it is chemically reduced in solution under low redox conditions. However, Co is one of the elements usually associated very strongly with Mn oxides (Murray, 1975b) because Co(II) can be oxidized to Co(III) on the surface of  $MnO_2$  (Murray and Dillard, 1979). Brewer and Spencer (1974) observed a maximum in dissolved Co in the top of the sulfide zone. They argued that this resulted because Co adsorbs on  $MnO_2$  particles that precipitate in the suboxic zone. These Mn–Co rich particles then sink and release Co upon dissolution of the Mn oxides when they are reduced by reaction with sulfide (Spencer et al., 1972; Brewer and Spencer, 1974; Haraldsson and Westerlund, 1991). Lewis and Landing (1992) argued that Co scavenged by Fe(III) particles may also be an important factor. Relatively high particulate Co concentrations were also observed by Tankere et al. (2001) in surface waters of the Black Sea where the influence of the Danube River inflow was strong.

We observed a strong maximum in particulate Co at the oxic–anoxic interface at Stn. R, the oxic–suboxic interface at Stn. T, and in the suboxic layer at Stn. G (Fig. 3.f). Increases in particulate Mn and Co at the upper part of suboxic zone (Fig. 3.c, f) suggest that Co is

cycling with Mn in this part of the water column. The Co/Al ratios at Stn. B were between the values for average crust and Turkish rivers (Fig. 4.f). The ratios at Stn. R were similar to the Turkish rivers down to the sulfide layer. They then increased approximately 100 times in the upper part of the sulfide zone. The surface samples at Stns. T and G were enriched in Co. At Stations T and G the Co/Al ratios in the suboxic zone are similar to those of Mn/Al but in addition they also increase in the sulfide zone. So it appears that Mn cycling does influence the distribution of particulate Co and that particulate enrichment of Co occurs in the sulfide zone as well.  $Co_{XS}$  and  $Mn_{XS}$  are strongly correlated when  $Mn_{XS}$  exceeds about  $1 \mu\text{g/L}$  (Fig. 6a) ( $r^2 = 0.995$ , Table 4). At lower values of  $Mn_{XS}$  there is no correlation.

#### 5.1.7. Molybdenum

Molybdenum exists in the Mo(VI) oxidation state and is conservative as  $MoO_4^{2-}$  in oxic seawater (Collier, 1985; Donat and Bruland, 1994). Because of the double negative charge, Mo would not be expected to adsorb strongly on negative surfaces (such as manganese dioxide) but nevertheless there is a strong correlation of Mo with Mn in manganese nodules and crusts (Murray and Brewer, 1977). The explanation is not clear but laboratory experiments do show that Mo has a strong affinity for adsorption on  $MnO_2$ . Under reducing conditions Mo might be reduced to the Mo(V) and/or Mo (IV) oxidation states (Bertine, 1972; Zheng et al., 2000). Removal as a mixed Mo–Fe–S precipitate occurs at low sulfide concentrations (Helz et al., 1996). Insoluble  $MoS_2$  can form at higher sulfide concentrations (Emerson and Husted, 1991). Helz et al. (1996) hypothesized that, in the presence of  $HS^-$ , one sulfur atom replaces an oxygen in the  $MoO_4^{2-}$  molecule, creating a complex that makes the Mo compound more likely to be bound to iron sulfides or humic-SH complexes.

The distribution of particulate Mo is similar to that of particulate Fe, especially at Stn. G (Fig. 3.g). All samples in the suboxic zone are enriched relative to lithogenic material; however, the Mo/Al ratios do not show clear cut evidence for Mn/Fe oxide scavenging (Fig. 4.g). The Mo/Al ratios show no excess Mo at Stn. B and increase progressively going from Stns. R to T to G. The surface samples may be elevated because of biological enrichment or anthropogenic inputs. There is an increase in the deepest samples that is most likely due to sulfide formation. Though previous studies suggested we might see a strong Mn–Mo correlation, we actually observed that  $Mo_{XS}$  correlated more strongly with  $Fe_{XS}$  (and  $Cr_{XS}$  and  $Ni_{XS}$ ) (Table 4). Though biological utilization of Mo is coupled to the marine nitrogen cycle (Stiefel, 1996), our data give no indication that the intense N cycling in the Black Sea influences the distribution of particulate Mo.

#### 5.1.8. Chromium

Vertical profiles of dissolved Cr in oxygenated sea water exhibit nutrient-type distributions (Murray et al., 1983). The main oxidation state of chromium under oxic conditions is Cr(VI), which is present as the soluble chromate anion ( $CrO_4^{2-}$ ). Cr(VI) is predicted to undergo reduction to Cr(III) under approximately the same redox conditions as manganese and nitrate (Rue et al., 1997). Some Cr(III) is produced in surface waters from biological and photochemical reduction and exists as hydrolyzed species (e.g.,  $Cr(OH)_3^+$ ) which is known to be strongly particle reactive. The tendency of being more soluble in the oxidized state and insoluble in the reduced state is the reverse of that seen for Mn, so Cr and Mn are not expected to correlate well in the particulate phase. In our data set  $Cr_{XS}$  and  $Mn_{XS}$  were negatively correlated (Table 4).

The vertical distribution of particulate Cr in the oxic waters shows an unambiguous surface enrichment relative to detrital particles. Apart from Stn. B, Cr has the highest concentration at Stn. G (Fig. 3.h). At this station the vertical profile from the surface to the deepest sample correlates well with Fe. At Station G the maximum is localized at around  $\sigma_\theta = 14.5$ , possibly due to the influence of particulate Fe scavenging at this density. The maximum for  $Cr_p$  at the transition station (T) is not as distinct as the maximum observed for  $Fe_p$ . However, Cr still has two broader maximum on the oxic–suboxic and suboxic–anoxic interfaces at this station. Cr/Al at Stn. B is close to the value for crust and rivers but the surface samples from Stns. R, T and G show Cr enrichments (Fig. 4.h). There is a small decrease in Cr/Al below the euphotic zone suggesting slow remineralization of Cr in the water column. Otherwise most of the samples from station R have ratios only slightly elevated over Turkish rivers. The Cr/Al ratios in all samples from Stns. T and G are elevated over rivers at all depths. There is some indication that the distributions of  $Cr_p$  are more like  $Fe_p$  than  $Mn_p$  in our samples. Oxidized Cr (like oxidized V) is possibly scavenged more strongly by iron oxides than by manganese oxides. However, for the data set as a whole,  $Cr_{XS}$  and  $Fe_{XS}$  are not strongly correlated.

#### 5.1.9. Vanadium

Vanadium is nearly conservative in aerobic seawater where it is present as anionic vanadate (e.g.,  $HVO_4^{2-}$  and/or  $H_2VO_4^-$ , Wehrli and Stumm, 1989). In the absence of oxygen, vanadate can be reduced to vanadyl, V(IV), which is probably present as the oxovanadium cation,  $VO^{2+}$  and/or  $VO(OH)_3^+$  (aq). Reduced V(IV) does not form strong sulfide species or solids but it does adsorb strongly onto particle surfaces. Both vanadate and vanadyl are scavenged by Mn and especially Fe oxyhydroxides (Wehrli and Stumm, 1989) but the smaller cationic vanadyl binds more strongly than the larger anionic vanadate. Because

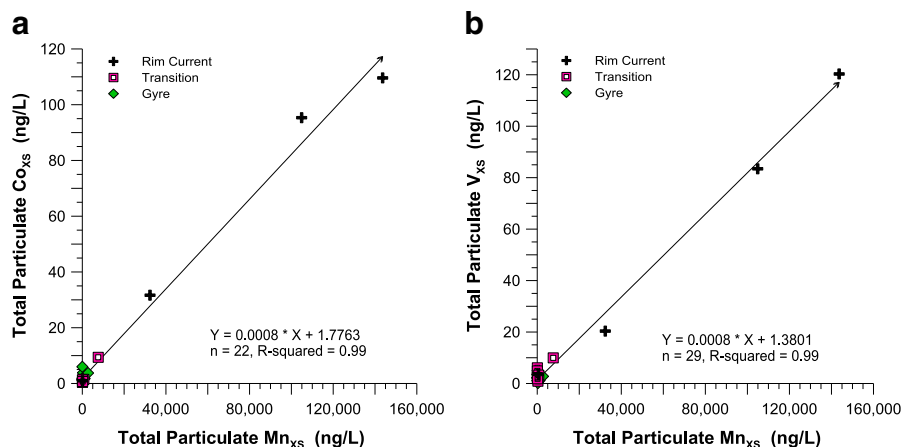


Fig. 6. Total particulate excess-Mn was plotted versus total particulate excess-Co (a) and excess-V (b) to show the correlations between these elements.

the V species are negatively charged they are often hypothesized to adsorb on Fe, rather than Mn, oxyhydroxides (Wehrli and Stumm, 1989). The explanation is that  $\text{MnO}_2$ , which has a  $\text{pH}_{(\text{ZPC})}$  near  $\text{pH} = 2.0$  (Murray, 1974), is negatively charged over most of the pH range but  $\text{FeOOH}$  has a  $\text{pH}_{(\text{ZPC})}$  around 7.5 (Balistrieri and Murray, 1981) so its surface charge is weaker and may be positive if the pH is less than 7.5. Experimental results suggest that V(V) can be reduced to V(III) under anoxic conditions by  $\text{H}_2\text{S}$  and forms  $\text{V}(\text{OH})_3(\text{s})$  (Wanty and Goldhaber, 1992), which may explain the observed enrichments under sulfate-reducing conditions (Wanty et al., 1990). In ocean profiles there is some evidence of depletion of dissolved V in the surface water, probably due to biological uptake (Collier, 1984).

The concentrations of particulate V decreased significantly (300–350 times at the surface) from the Bosphorus (B) to the Gyre station (G) (Fig. 3.i). The V/Al at Stn. B was very similar to the value for rivers (Fig. 4.i). Three of the surface samples ( $\sigma_\theta = \sim 11.6$ ) from Stns. T and G had excess V that may be due to biological enrichment. Excess V is also seen in the samples from 150 m ( $\sigma_\theta = \sim 16.4$ ) at Stn. R and in some of the samples in the suboxic zone at Stns. T and G. The fact that maximum V/Al ratios occur in the suboxic zone at the same densities as Mn/Al and Fe/Al suggests that scavenging of V by Fe and Mn oxyhydroxides is an important process occurring there. The resolution of our samples does not allow us to distinguish whether this is mainly by Mn or Fe oxides and  $\text{V}_{\text{XS}}$  correlated strongly with both  $\text{Mn}_{\text{XS}}$  (0.997) (Fig. 6b) and  $\text{Fe}_{\text{XS}}$  (0.798) (Table 4). V does not form sulfide minerals so the high V/Al ratios in the upper sulfide zone at Stn. G suggests scavenging of reduced V(III) on new sulfide particles.

#### 5.1.10. Nickel

Nickel has only one oxidation state in seawater (Ni(II)) and a relatively uncomplicated solution chemistry. It does not adsorb strongly on metal oxides and other surfaces (Murray, 1975a). Its profiles in the open ocean reflect nutrient like behavior (Bruland, 1980). Thus, its distributions are well correlated with nitrate, phosphate and silica but the correlations are often not as strong as observed for Cd and Zn (Bruland, 1980; Saager et al., 1992). Piper and Calvert (2009; in press) argued that Ni may be a master trace element proxy for the settling flux of organic matter out of the euphotic zone (export production).

Ni in the Black Sea was studied in detail by Brewer and Spencer (1974), Haraldsson and Westerlund (1988, 1991) and Lewis and Landing (1992). Haraldsson and Westerlund (1988) concluded that Ni does not appear to be affected by the appearance of sulfide.

Our particulate Ni ( $\text{Ni}_p$ ) concentrations (Fig. 3.j) were much higher at the Bosphorus station than the offshore stations as also seen by Tankere et al. (2001).  $\text{Ni}_p$  has a profile somewhat similar to  $\text{Fe}_p$  except that the variations in  $\text{Fe}_p$  are larger and for a large Fe maximum at the lower boundary of the oxic layer at Stn. T and another smaller Fe maximum in the suboxic layer at Stn. G. The enrichments of  $\text{Ni}_p$  (Fig. 4.j) and  $\text{Fe}_p$  (Fig. 4.d) at a density of  $\sigma_\theta = 14.2$  are similar. The deepest sample at Stn. G is enriched in both Fe and Ni.  $\text{Ni}_{\text{XS}}$  had significant correlations with  $\text{Cr}_{\text{XS}}$  and  $\text{Mo}_{\text{XS}}$  but not with  $\text{Mn}_{\text{XS}}$  or  $\text{Fe}_{\text{XS}}$  (Table 4).

The particulate Ni/Al ratios at Stn. B and surface samples of Stn. R are very close to the values for Turkish rivers. The surface samples at Stns. T and G have 5–10 fold enrichment relative to rivers. There is no evidence of Ni remineralization below the euphotic zone.

#### 5.1.11. Barium

Barium (Ba(II)) is an alkaline earth class A metal. This means that it forms strong solution complexes with  $\text{SO}_4^{2-}$ ,  $\text{CO}_3^{2-}$  and  $\text{OH}^-$  and does not form sulfide complexes or solid phases. In the open ocean, dissolved Ba correlates with silicate and alkalinity (Bacon and Edmond, 1972; Chan et al., 1977) in what is referred to as a deep regeneration cycle (Bruland, 1980), but not because Ba is taken up by  $\text{SiO}_2$  minerals.

Instead  $\text{Ba}^{2+}$  appears to form  $\text{BaSO}_4$  crystals in microzones of decaying biogenic particles (Bishop, 1988). These barite crystals sink into the deep water where they slowly re-dissolve to result in a deep regeneration cycle (Dymond et al., 1992).

Ba distributions in anoxic water columns also appear to be controlled by barite formation and regeneration (Fig. 3.k). Falkner et al. (1993) compared distributions of dissolved and particulate Ba, Fe, and Mn and suggested that the maximum of  $\text{Ba}_p$  did not result from adsorption onto freshly precipitated Fe and/or Mn oxyhydroxides. They proposed that microbial activity near the redox interface in the Black Sea promoted the breakdown of settling particulate matter resulting in the release of barite just above the  $\text{O}_2/\text{H}_2\text{S}$  interface, thus providing a source for the observed suspended particulate maxima (Falkner et al., 1993).

We observed that the concentrations of particulate Ba were enriched in the surface waters of all stations (Fig. 3.k).  $\text{Ba}_p$  decreased to minimum values at around  $\sigma_\theta = 14$ , at Stns. R, T, and G, as seen for particulate P. Small maxima in  $\text{Ba}_p$  were observed at the vicinity of the redox interface at Stn. R and at the onset of the sulfide layer at Stns. T and G.

Ba/Al ratios at Stn. B were close to average crust and Turkish rivers (Fig. 4.k). Excess Ba was observed in surface samples at Stns. R, T and G, consistent with biological enrichment. The Ba/Al ratios decreased below the euphotic zone at Stns. R, T and G suggesting remineralization of  $\text{Ba}_p$ . The Ba/Al ratios at Stn. G are always enriched relative to all lithogenic sources except the few deepest anoxic samples. Excess Ba exists in the suboxic zone at Stns. T and G, possibly due to  $\text{MnO}_2$  sorption. Ba has been shown to be adsorbed fairly strongly by  $\text{MnO}_2$  (Murray, 1975a). Thus we differ from Falkner et al. (1993) and suggest that  $\text{Ba}_p$  distributions might be influenced by adsorption/uptake onto Mn and Fe oxyhydroxides formed in the vicinity of the redox interfaces of the Black Sea. Excess  $\text{Ba}_p$  decreases into the sulfide zone which is consistent with the fact that  $\text{Ba}_p$  should decrease when sinking Mn/Fe oxides are reduced and Ba is not expected to form sulfide minerals. However, for our data set as a whole,  $\text{Ba}_{\text{XS}}$  had no significant positive correlations with other elements (Table 4). The largest correlation was a negative correlation with  $\text{Ti}_{\text{XS}}$  which suggests  $\text{Ba}_{\text{XS}}$  may be a tracer for non-lithogenic material.

#### 5.1.12. Copper

Cu is a class B transition metal and its speciation in seawater is dominated by Cu(II). The major inorganic species are  $\text{CuCl}^+(\text{aq})$ ,  $\text{CuCO}_3^\circ$ ,  $\text{Cu}(\text{OH})^+$  and  $\text{Cu}^{2+}$ . Cu also forms strong complexes with organic matter and has a strong biological affinity. Cu shows nutrient-like properties in oxic seawater, but is also influenced by scavenging processes in the ocean water column (Boyle et al., 1977). Calculations suggest that it may be reduced to Cu(I) under reducing conditions (Emerson et al., 1983) and form sulfide phases such as  $\text{CuS}(\text{s})$  and/or  $\text{Cu}_2\text{S}(\text{s})$  (Brewer and Spencer, 1974; Jacobs and Emerson, 1982; Jacobs et al., 1985, 1987; Haraldsson and Westerlund, 1991).

Previous work has found that dissolved Cu concentrations are high in the surface waters of the Black Sea, then decrease near the sulfide interface. Dissolved Cu concentrations are very low in the deep water (Lewis and Landing, 1992). Muller et al. (2001) suggested that a significant portion of Cu in the central surface waters of the Black Sea originated from the western shelf.

In this study, the highest concentrations of particulate Cu were observed at the Bosphorus station (Stn. B) (Fig. 3.l). The  $\text{Cu}_p$  concentrations at Stns. R, T, and G were pretty uniform through the oxic layer and most of the suboxic zone. They increased sharply in the lower suboxic zone ( $\sigma_\theta = 15.9$  to  $16.1$ ) and then decreased with depth as sulfide increased. This pattern was sufficiently different from those of Mn and Fe suggesting that Mn and Fe oxides and redox cycling have little effect on Cu distributions. Similar maxima were observed by Haraldsson and Westerlund (1991) and they attributed it to formation of organic matter at the bottom of the suboxic zone.

In general, the particulate Cu/Al ratio was enriched relative to detrital material (Fig. 4.l). The exception was the Bosphorus station, which had the highest concentrations but had a Cu/Al very similar to the values for average crustal and Turkish rivers. At Stations R, T and G, Cu/Al ratios in surface waters were enriched by 5 to 10 times relative to Turkish rivers. Maximum enrichment factors occurred just above the sulfide interface. The decrease of Cu/Al in the sulfide layer at Stn. G suggests that in situ particle formation due to metal-sulfide scavenging was not important. Nevertheless the Cu/Al ratios remain enriched by 10 fold relative to crust and Turkish rivers. The only significant correlation of  $Cu_{XS}$  was with  $Ag_{XS}$  (Table 4).

#### 5.1.13. Zinc

Zinc (also a class B metal) has only one oxidation state in seawater (Zn(II)) and has nutrient like distributions. It also forms strong organic complexes (Muller et al., 2001). It does not change its oxidation state under reducing conditions but it does form sulfide minerals (Brewer and Spencer, 1974; Lewis and Landing, 1991; Haraldsson and Westerlund, 1991). Spencer et al. (1972) observed that particulate Zn concentrations in the Black Sea increased to maximum values at 35 m below the oxic-anoxic interface. They attributed this to formation of Zn sulfide precipitates resulting from the downward flux of Zn by eddy diffusion. However, according to Lewis and Landing (1991), Zn is greatly undersaturated throughout the water column with regard to all hydroxide, carbonate and sulfide solid phases. Detrital silicates also have a recognizable influence on  $Zn_p$  distributions (Spencer et al., 1972).

Our particulate Zn concentrations agreed well with those reported previously (Brewer and Spencer, 1974; Haraldsson and Westerlund, 1991; Lewis and Landing, 1992) (Fig. 3.m). The exception is the Zn maximum located at  $\sigma_\theta = 15.4$  at the Gyre station. This depth exhibits higher Zn concentrations and Zn/Al enrichment (Fig. 4.m) relative to other samples taken from the oxic layer. Otherwise, the lack of particulate Zn maxima in the suboxic layer indicates that this element is not being co-precipitated, or adsorbed, to any great extent on the Mn/Fe oxides that form there particularly at Stns. T and G.

The Zn/Al ratios show no enrichment at Stn. B relative to average crust or Turkish rivers (Fig. 4.m). The surface samples at Stns. R, T, and G are all enriched. Almost all samples below the euphotic zone are enriched in Zn relative to Turkish rivers with the exception of one sample from Stn. T at  $\sigma_\theta = 14.2$ . There was no clear enrichment that could be specifically attributed to sorption by Mn/Fe oxides or sulfides. The Zn/Al increase from suboxic to sulfide at Stns. R, T, and G, consistent with sulfide formation.

Anthropogenic contamination could be a factor. The Zn/Al ratio in the Danube sample was significantly larger than in Turkish rivers and average crust (Yiğiterhan and Murray, 2008). This was also seen for the Me/Al ratios of Pb, Ag, Cu, and Cd. We suspect that this may also reflect anthropogenic contamination in the Danube River basin. In our data set we observed that  $Zn_{XS}$  had significant negative correlation with  $Ti_{XS}$  ( $-0.829$ ) (Table 4), which may be suggesting that  $Zn_{XS}$  may also be a tracer for non-lithogenic material similar to  $Ba_{XS}$ .

#### 5.1.14. Cadmium

Cadmium is a class B metal that occurs in one main oxidation state (Cd(II)). Its main inorganic species in seawater are the chloro complexes,  $CdCl_2^\circ$  and  $CdCl^+_{(aq)}$  (Bruland, 1983). Cd has a nutrient like distribution in the open ocean and its strong correlation with  $PO_4^{3-}$  has been used to reconstruct paleo nutrient distributions (Boyle, 1988). In the presence of sulfide Cd(II) forms soluble sulfide complexes and insoluble sulfide solid phases ( $CdS_{(s)}$ ) (Stumm and Morgan, 1981; Gobeil et al., 1997). Tankere et al. (2001) observed an increase of dissolved Cd concentrations gradually with depth in the upper layer of the Black Sea and attributed this as the coupling of Cd with the cycle of production and decomposition of organic matter. They observed a good correlation between dissolved Cd and nutrients

( $NO_3^-$ ,  $NO_2^-$ ,  $PO_4^{3-}$ ,  $Si(OH)_4$ ). The concentrations of dissolved Cd in the sulfidic layer are significantly lower than in the oxic layer (Haraldsson and Westerlund, 1991).

We observed high surface concentrations of particulate Cd (Fig. 3.n) at Stns. R, T, and G; which could result from biological uptake of dissolved Cd or anthropogenic contamination. The concentration of particulate Cd at Stn. B was approximately 20–30 fold higher than at Stns. R, T, and G. The  $Cd_p$  concentrations in surface water were very similar at the three offshore stations.  $Cd_p$  increased sharply at the oxic-anoxic interface at Stn. R, and at the suboxic-anoxic boundary at Stns. T and G. This is most likely due to formation of sulfide precipitates (Haraldsson and Westerlund, 1991).

Surface concentrations of  $Cd_p$  were high at all four stations. However the Cd/Al ratios show that the Cd/Al ratio at Stn. B has the crustal ratio. At Stns. R, T and G the Cd/Al ratios show enrichment of Cd relative to crust. The higher enrichments of the Cd/Al ratio at Stns. G and T relative to Danube and Turkish rivers suggests more intense biological uptake of dissolved Cd (Cullen et al., 1999). However it is difficult to rule out anthropogenic contamination. The Cd/Al ratio is much higher in Danube River suspended matter than in samples from Turkish rivers (Fig. 4.n) (Yiğiterhan and Murray, 2008). The particulate Cd/Al ratios at Stns. R, T, and G increase sharply at the top of the sulfide zone just below  $\sigma_\theta = 16.0$  (Fig. 4.n). This supports the possibility of Cd-sulfide precipitation for removal of dissolved Cd from the water column (Lewis and Landing, 1992). The amount of  $Cd_{XS}$  is probably controlled by several processes through the water column (i.e. production and decomposition of biogenic particles, pollution, sulfide formation; Tankere et al., 2001) which is probably the reason why  $Cd_{XS}$  had no significant correlations (Table 4).

#### 5.1.15. Silver

Ag exists in only one oxidation state (Ag(I)) and the speciation in oxic seawater is dominated by chloro-complexes ( $AgCl^\circ$  and  $AgCl_2^-$ ) (Bruland, 1983). In the presence of sulfide, Ag forms a wide variety of dissolved sulfide complexes and insoluble sulfide solid phases (Stumm and Morgan, 1981). The concentrations of dissolved silver (Ag) in open ocean waters are extremely low (Martin et al., 1983), due mainly to its high particle reactivity and low crustal abundance (Bruland, 1983). McKay and Pedersen (2008) suggested that dissolved Ag may be scavenged to particles by precipitation as  $Ag_2S(s)$  in microenvironments within settling decaying organic matter. Kramer et al. (2011) recently suggested that Ag is associated with biogenic opal. Anomalously high Ag concentrations can be a strong indicator of sewage contamination (especially photographic industry waste) and have been used as tracers of point source waste water discharges (Sañudo-Wilhelmy and Flegal, 1992). The Danube River suspended matter had an elevated Ag/Al ratio relative to crust which is consistent with anthropogenic contamination (Yiğiterhan and Murray, 2008). There are no previous data for Ag concentrations in the Black Sea.

In our data set the concentration of particulate Ag ( $Ag_p$ ) was highest in the Bosphorus and decreased to the offshore sampling stations.  $Ag_p$  in the surface samples at the Stns. R, T, and G were very comparable but were about 20 times lower than at Stn. B (Fig. 3.o). Though the  $Ag_p$  concentration was high at Stn. B the Ag/Al ratio fell close to the Ag/Al ratio given for Turkish rivers (Fig. 4.o), thus  $Ag_p$  appears to be detrital.

A depletion of  $Ag_p$  was observed for Stns. G, T, and R at  $\sigma_\theta = 14.1$  to 14.5. In this density range,  $Ag_p$  concentrations decrease to a minimum, yet Ag/Al ratios are slightly elevated. Below this depth  $Ag_p$  increases to another small secondary maximum that occurs just above the oxic-anoxic interface at Stn. R, and above the suboxic-anoxic interface at Stns. T and G.  $Ag_{XS}$  did not have significant correlations with the other class B elements (Pb, Cd, Zn, Cu) (Table 4).

All of our samples are enriched in Ag relative to Turkish rivers and crust which suggests input of contaminated particles from the Danube

River. It could be that the entire upper water column of the Black Sea is contaminated with Ag of anthropogenic origin.

#### 5.1.16. Lead

Lead is a class B metal that occurs in the Pb(II) oxidation state. It forms a variety of carbonate and chloride complexes in oxic seawater (Bruland, 1983). As a class B metal, Pb forms dissolved and particulate sulfide species (Stumm and Morgan, 1996). Pb is thought to adsorb strongly on particle surfaces. Haraldsson and Westerlund (1991) observed that the concentrations of particulate Pb<sub>p</sub> increased as total Pb decreased due to the formation of particulate Pb sulfides. Wei and Murray (1994) studied the distribution of <sup>210</sup>Pb in the Black Sea and observed an increase in particulate <sup>210</sup>Pb and the particulate/dissolved ratio (K<sub>D</sub>) in the sulfide layer. Tankere et al. (2001), observed no increase in Pb concentrations in the sulfide layer which suggested that sulfide formation was not an important mechanism. On the other hand, Lewis and Landing (1991) observed some Pb<sub>p</sub> enrichments relative to crust in the anoxic waters of the Black Sea and suggested this was most likely due to metal-sulfide scavenging and/or precipitation of some Pb-sulfide solid phase. The Pb/Al ratio in Danube River particulate matter was 100 fold higher than crust or Turkish rivers, probably because of anthropogenic input (Yiğiterhan and Murray, 2008). High Pb concentrations of anthropogenic origin were also found by Tankere et al. (2001) in the Danube plume.

In our data set Pb<sub>p</sub> and Ag<sub>p</sub> were similar in many ways. For both elements the particulate concentrations were highest at Stn. B (Fig. 3.p), yet the ratios to Al were close to crust (Fig. 4.p). Pb<sub>p</sub> concentrations were similar at Stns. R, T, and G yet the Pb/Al ratio increased from R to T to G. Pb<sub>p</sub> had maxima at the oxic-anoxic interface of Stn. R but Stns. T and G had lower Pb<sub>p</sub> and no maxima in the suboxic zone. Pb<sub>p</sub> increased with depth in the sulfide zone which may be due to increased scavenging of Pb by sulfide precipitation.

The Pb/Al ratio at Stn. B is close to the ratio in Turkish rivers and average crust (Fig. 4.p). But all other samples from the Black Sea (surface, suboxic and sulfidic from Stns. R, T, and G) were uniformly enriched in Pb relative to lithogenic material. In general the Pb/Al ratios follow the sequence of G>T>R. The reason can be decreasing amount of terrestrial, aluminosilicate containing particles moving from Stn. R to G. Despite the suggestions that Pb<sub>XS</sub> may be an indication of pollution, its significant correlations were with tracers of metal oxide cycling (Mn<sub>XS</sub>, Fe<sub>XS</sub>, V<sub>XS</sub>, Co<sub>XS</sub>) rather than other elements of possible anthropogenic origin (e.g., Ag<sub>XS</sub>, Cd<sub>XS</sub>, Zn<sub>XS</sub>) (Table 4).

## 5.2. Surface layer metal enrichments

Several elements are enriched in the surface layers of the Black Sea. These surface enrichments could arise from biological uptake into particles or from input of contaminated particles from rivers. It is difficult to distinguish between these sources as many of the elements known to have an anthropogenic origin also have a tendency to be enriched by biological processes. We will examine each of these possibilities separately.

### 5.2.1. Biological enrichment

Plankton concentrate trace metals by several mechanisms including active nutrient uptake and sorption on the surfaces of their cells. Thus they typically have higher metal concentrations (when normalized to Al) relative to seawater and lithogenic material (e.g., Fraustu da Silva and Williams, 1991). In some cases metals are enriched because they have essential biological functions. In other cases the reasons for the enrichments are unclear. These metal enrichments and vertical transport of elements by sinking particles are important for marine biogeochemical cycles (Martin and Knauer, 1973). However, except for a few notable studies (e.g., Martin and Knauer, 1973;

Martin et al., 1976; Collier and Edmond, 1984; Kuss and Kremling, 1999; Ho et al., 2003, 2007; Twining et al., 2004, 2010, 2011), the elemental composition of plankton is still poorly known.

A subset of our surface samples was appropriate for calculating the excess metal concentrations. These samples were from the surface waters of Stns. R, T, and G where the total suspended matter was dominated by bulk plankton, as represented by particulate P (Fig. 5). The fluorescence data from the rosette casts were used as a criterion for selecting samples. These samples were from density values of about  $\sigma_{\theta} = 11.55$  to 11.98, which correspond to euphotic zone depths at Stns. R (20 and 35 m), T (10 and 23 m) and G (10 m) (Table 5). The surface samples from the Bosphorus station (Stn. B) had extremely high concentrations of particulate P, which were uniform with depth (not plotted) and most likely result from local pollution. These samples were not included in this analysis.

Excess metal concentrations (Me<sub>XS</sub>) were calculated by subtracting the lithogenic material from the measured total particulate metal concentrations as described earlier. We then calculated the ratios of Me<sub>XS</sub> to P for comparison with previous studies of biological enrichment Phosphorus was used as a proxy for biomass because our filters were made of carbon which precluded use of carbon directly.

The Me<sub>XS</sub>/P values for Stns. R, T, and G (mmol/mol) calculated using this approach are summarized in Table 5. The Me/P ratios in surface samples from the Black Sea are compared with previous estimates of metal compositions of plankton (also calculated as Me/P) from Martin and Knauer, 1973; Martin et al., 1976; Collier and Edmond, 1984; Bruland et al., 1991; Kuss and Kremling, 1999; Ho et al., 2003, 2007, and Twining et al., 2004, 2010, 2011. Many of these previous studies did not include Al analyses thus the literature values used in this comparison are based on total metal, rather than excess Me composition. In addition, the previous studies needed to include P data to be included in this comparison. For many elements (e.g. Ti, V, Cr, Ag, Ba, Pb, U) we could find no previous Me/P data thus we can only compare Me/P ratios with previous studies for about half of the metals we analyzed. For those cases where we can make this comparison we see that the Me/P ratios from the Black Sea tend to be much higher. This comparison clearly shows that the lithogenic correction is insufficient to account for all the nonbiological particulate metals in the samples. The ratios from the Black Sea are much higher than in previous open ocean studies for Cu, Zn, Mo and Ni in marine plankton. For Cd and Co the ratios are comparable. Even after you correct for the terrigenous fraction using Me/Al ratios from rivers there is usually much more Me/P than seen in previous open ocean data sets of plankton composition.

### 5.2.2. Anthropogenic impacts

Several recent studies have shown that some elements like Pb, Zn, Cu, Ag, and Cd have especially high concentrations in samples from the three main branches of the Danube River delta and tributaries (Literathy and Laszlo, 1999; Ricking and Tertyze, 1999; Guieu and Martin, 2002), and this result is consistent with anthropogenic contamination. Yiğiterhan and Murray (2008) used Me/Al ratios to argue that high values seen for several trace elements in the Danube suggest more contamination than for the Turkish rivers. The Danube River was especially enriched in Ag, Pb, Zn, Cd and Cu. These five elements are well known indicators of pollution.

In this study of suspended matter in the Black Sea we see that Me/Al ratios of Pb (Fig. 4p), Ag (Fig. 4o), Cd (Fig. 4n), Zn (Fig. 4m), and Cu (Fig. 4l) are generally high in the surface layer and similar to the Me/Al ratios for the Danube River. A confusing aspect of this argument in favor of pollution is that the highest concentrations were usually seen in samples from the Bosphorus (Stn. B) but the Me/Al ratios were usually in good agreement with crust and Turkish rivers, instead of the Danube. Another complication is that the highest Me/Al ratios tended to be highest at Stns. T and G which are furthest away from the Danube source. There are many sources of Me that are not associated

**Table 5**  
Comparison of elemental composition of the Black-Sea non-lithogenic suspended particles (this study<sup>a</sup>) with plankton cultivated (Ho et al., 2003; 2007), collected (others) from the coastal and open oceans, and average crustal ratios (Taylor, 1964). All excess particulate trace metal (Me) concentrations are quoted normalized to phosphate (P) and have the same unit: mmol-Me/mol-P.

Me <sub>Xs</sub> /P ratio	Stn. R	Stn. R	Stn. T	Stn. T	Stn. G	Stn. G	This Study	Martin and Knauer	Martin et al.	Collier and Edmond	Kuss and Kremling	Twining et al.	Twining et al.	Twining et al.	Ho et al.	Ho et al.	Ho et al.	Taylor
	<sup>1</sup> 20m <sup>a</sup>	<sup>1</sup> 35m <sup>a</sup>	<sup>2</sup> 10m <sup>a</sup>	<sup>2</sup> 23m <sup>a</sup>	<sup>3</sup> 10m <sup>a</sup>	<sup>3</sup> 30m <sup>a</sup>	<sup>4</sup> Average	<sup>5</sup> 1973	<sup>6</sup> 1976	<sup>7</sup> 1984	<sup>8</sup> 1999	<sup>9</sup> 2004a	<sup>10</sup> 2010	<sup>11</sup> 2011	<sup>12</sup> 2003	<sup>13</sup> 2007	<sup>14</sup> 2007	<sup>15</sup> 1964
Th <sub>Xs</sub> /P	<-42.5>	<-42.8>	<-5.3>	<-6.4>	<-13.7>	4.2	4.2	-	-	-	0.7	-	-	-	-	121	16.1	3515
V <sub>Xs</sub> /P	0.3	<-1.1>	2.2	2.1	1.0	<-0.1>	1.4	-	-	-	-	-	-	-	-	9.3	0.68	78.2
Cr <sub>Xs</sub> /P	20.2	21.9	13.9	33.8	110	150	58.3	-	-	-	-	-	-	-	-	-	-	56.7
Mn <sub>Xs</sub> /P	<-62.10>	<-15.930>	18.270	21.170	18.670	227.900	71.510	0.38	0.38	0.52	1.59	0.24	0.65	0.62	3.8	149	9.3	510
Fe <sub>Xs</sub> /P	<-391>	<-394>	<-11.4>	2.1	94.5	401	166	5.2	5.0	11.1	4.5	0.63	5.0	2.6	7.5	6520	323	29,740
Ni <sub>Xs</sub> /P	2.4	<-0.3>	3.7	9.4	26.0	12.9	10.9	0.21	0.35	0.75	0.88	0.53	2.2	0.67	-	5.0	1.4	37.7
Co <sub>Xs</sub> /P	0.21	<-0.06>	0.13	0.17	0.95	2.5	0.79	0.20	0.20	0.20	0.20	-	-	0.10	0.19	2.9	0.35	12.5
Cu <sub>Xs</sub> /P	6.7	2.4	4.4	9.3	10.7	21.5	9.2	0.18	0.38	0.78	0.42	-	-	-	0.38	6.8	4.8	25.5
Zn <sub>Xs</sub> /P	34.9	17.2	8.6	7.3	25.7	18.2	18.7	0.84	1.8	7.4	1.5	3.9	12.0	2.1	0.80	32.7	10.7	31.6
Mo <sub>Xs</sub> /P	0.70	0.62	0.91	0.55	6.4	0.90	1.7	-	-	-	-	-	-	-	0.03	-	-	3.5
Ag <sub>Xs</sub> /P	0.02	0.03	0.04	0.08	0.05	0.17	0.07	-	-	-	-	-	-	-	-	-	-	0.02
Cd <sub>Xs</sub> /P	0.23	0.19	0.21	0.20	0.41	0.17	0.23	0.07	0.46	0.71	0.53	-	-	0.21	-	-	-	0.05
Ba <sub>Xs</sub> /P	182	135	107	144	497	17	180	-	-	1.05	-	-	-	-	-	-	-	91.3
Pb <sub>Xs</sub> /P	1.8	1.5	1.0	1.2	4.1	26.2	6.0	-	-	-	-	-	-	-	-	-	-	1.8
U <sub>Xs</sub> /P	0.009	0.003	0.007	0.003	0.009	0.002	0.006	-	-	-	-	-	-	-	-	-	-	0.335

<sup>a</sup> Total non-lithogenic suspended particles (>1 μm pore size) from the Black Sea rim current<sup>1</sup>, transition to open<sup>2</sup>, center of western gyre<sup>3</sup> stations, <sup>4</sup>Average of six samples from the Black Sea, <sup>5</sup>North Pacific Monterey Bay, <sup>6</sup>North Pacific, Stn. 54–88, <sup>7</sup>Average of bulk plankton from Antarctic, Galapagos, Central Tropical Pacific, <sup>8</sup>Biogenic samples from NE Atlantic, <sup>9</sup>Average of diatom, autotrophic flagellates and heterotrophic plankton from Southern Ocean, <sup>10</sup>Average of three mesoscale eddies in the Sargasso Sea, <sup>11</sup>Average of bulk, diatom, autotrophic flagellates, heterotrophic flagellates, and pico plankton from Equatorial Pacific, <sup>12</sup>Average culture, <sup>13</sup>Southern China Sea Pearl River mouth 2–30 m depth interval, <sup>14</sup>S.E. Asia time-series site 25–200 m depth interval, <sup>15</sup>Average crustal ratios (– = Not reported; <-> = negative values).

with Al. For example, aerosols from Europe with non-lithogenic metal content. This might include particles from such as soot from fires and coal burning. Contributions of these particles are not included here due to lack of data.

## 6. Conclusions

The concentrations of total particulate metal concentrations were determined at four stations in the southwestern region of the Black Sea. The particulate matter in the water column is influenced by lithogenic input from rivers, biological processes and geochemical processes. Our analyses included a suite of redox-sensitive metals, including Cu, Cr, Cd, Mo, Re, U, and V. Mn, Fe, Ba, Ni, Pb, Zn, Co, Ti, Al, and P that were analyzed to provide information about redox state and input of biogenic and terrigenous material.

Particulate matter compositions showed large spatial variations. Al (a tracer for lithogenic detrital material) which decreased from the Bosphorus (Station B) to the Rim Current (Station R) to the Transition (Station T) to the center of the western Gyre (Station G). Almost all the other elements had much higher concentrations at the Bosphorus station (Station B). However these samples had Me/Al ratios that were virtually identical to the average Crust and Turkish rivers, even though the source of this water is surface water from the southwestern Black Sea. The Rim Current station (Stn. R) tended to have higher concentrations than the Transition and Gyre stations (Stns. T and G) for many elements, including Al, Ti, Fe, U, V, Zn, Ag, and Pb. Mn (more so than Fe) tended to have higher values in the suboxic zone at density values of  $\sigma_t = 15$  to  $\sigma_t = 16$  and then decreased to lower concentrations after the first appearance of sulfide at  $\sigma_t > 16$ . In general, the compositions at the Transition and Gyre stations tended to be similar. Elements influenced by sulfide formation in the anoxic layer at density values greater than  $\sigma_t = 16$  included Fe, Cr, Ni, Co, Mo, and possibly Ag.

Redox cycling in the suboxic zone was observed, as expected, for Mn and Fe. The Fe/Mn oxides that form play an important role in scavenging other metals. Elements that appeared to be influenced by Fe/Mn oxides scavenging were U, V, Ni, Co, Cu, Zn, and Ba.

Surface samples were enriched in particulate P and several trace elements. Average concentrations of excess Me ( $Me_{XS} = Me_{Total} - Me_{Lithogenic} = Me_{Total} - [(Me/Al)_{TR} \times Al_{Total}]$ ) decrease in the sequence of Ba > Fe > Cr > Mn > Zn > Ni > Cu > Mo > V > Co > Cd > U for the overall sample set. The ratios of  $Me_{XS}/P$  in these surface samples were much higher than Me/P ratios observed in previous studies of open ocean plankton. The lithogenic corrections were insufficient to account for all the nonbiological metals. Anthropogenic contamination of the surface layer of the Black Sea may be the explanation.

Supplementary materials related to this article can be found online at doi:10.1016/j.marchem.2011.05.006.

## Acknowledgements

We gratefully acknowledge extensive education on analytical technique and assistance in the lab and at sea from Barbara Paul. Semal Yemenicoglu, Laurie Balistrieri, Ann Bucklin and Clara Fuchsman helped with many different stages of this project. Robert Anderson provided the 1988 sediment sample used as an internal standard. We also would like to thank to anonymous reviewers for their valuable comments and suggestions. This research was supported by NSF Grants OCE0081118; MCB-0132101 and INT-0137601. Dr. Yigiterhan benefitted from TUBITAK NATO A-2 Fellowship and Grant 101Y105.

## References

- Anderson, R.F., LeHuray, A.P., Fleischer, M.Q., Murray, J.W., 1989. Uranium deposition in Saanich Inlet sediments, Vancouver Island. *Geochimica et Cosmochimica Acta* 53, 2205–2213.

- Anderson, R.F., Fleischer, M.Q., Lyons, T., Cowie, G., 1991. Sedimentary record of a shoaling of the oxic/anoxic interface in the Black Sea. *EOS, Transactions, American Geophysical Union* 72 (51), 36–37.
- Bacon, M.P., Edmond, J.M., 1972. Barium at GEOSEC III in the Southwest Pacific. *Earth and Planetary Science Letters* 16, 66–74.
- Balistrieri, L.S., Murray, J.W., 1981. The surface chemistry of goethite ( $\alpha$ -FeOOH) in major ion sea water. *American Journal of Science* 281, 788–806.
- Balistrieri, L.S., Murray, J.W., 1982a. The surface chemistry of  $\delta$ MnO<sub>2</sub> in major ion sea water. *Geochimica et Cosmochimica Acta* 46 (6), 1041–1052.
- Balistrieri, L.S., Murray, J.W., 1982b. The adsorption of Cu, Pb, Zn, and Cd on goethite from major ion seawater. *Geochimica et Cosmochimica Acta* 46 (7), 1253–1265.
- Bargar, J.R., Tebo, B.M., Bergmann, U., Webb, S.M., Glatzel, P., Chiu, V.Q., Villalobos, M., 2005. Biotic and abiotic products of Mn(II) oxidation by spores of the marine *Bacillus* sp. strain SG-1. *American Mineralogist* 90, 143–154.
- Bertine, K.K., 1972. The deposition of molybdenum in anoxic water. *Marine Chemistry* 1, 43–53.
- Bevington, P.R., Robinson, D.K., 1992. *Data Reduction and Error Analysis for the Physical Sciences*, 2nd edition. McGraw Hill, 328 pp.
- Bishop, J., 1988. The barite-opal-organic carbon association in oceanic particulate matter. *Nature* 332, 341–343.
- Boyle, E.A., 1988. Cadmium: chemical tracer of deep-water paleoceanography. *Paleoceanography* 3, 471–490.
- Boyle, E.A., Sclater, F., Edmond, J.M., 1977. The distribution of dissolved copper in the Pacific. *Earth and Planetary Science Letters* 37, 38–54.
- Brewer, P.G., Spencer, D.W., 1974. Distribution of some trace elements in Black Sea and their flux between dissolved and particulate phases. In: Degens, E.T., Ross, D.A. (Eds.), *The Black Sea-Geology, Chemistry and Biology*. : Memoirs of the American Association of Petroleum Geologists, vol. 20. American Association of Petroleum Geologists, Tulsa, Oklahoma, USA, 137–143.
- Bruland, K.W., 1980. Oceanographic distributions of cadmium, zinc, nickel, and copper in the North Pacific. *Earth and Planetary Science Letters* 47, 176–198.
- Bruland, K.W., 1983. Trace elements in seawater. In: Riley, J.P., Chester, R. (Eds.), *Chemical Oceanography*, 8. Academic Press, New York, pp. 157–221.
- Bruland, K.W., Donat, J.R., Hutchins, D.A., 1991. Interactive influences of bioactive trace metals on biological production in oceanic waters. *Limnology and Oceanography* 36, 1555–1577.
- Burton, J.D., Stratham, P.J., 1988. Trace metals as tracers in the ocean. *Philosophical Transactions of the Royal Society of London* 325, 127–145.
- Calvert, S.E., Pedersen, T.F., 1993. Geochemistry of recent oxic and anoxic marine sediments: Implications for the geological record. *Marine Geology* 113, 67–88.
- Calvert, S.E., Pedersen, T.F., 2007. Elemental proxies for paleoclimatic and paleoceanographic variability in marine sediments: interpretations and application. In: Hillaire-Marcel, C., de Vernal, A. (Eds.), *Paleoceanography of the Late Cenozoic. Part 1. Methods of Late Cenozoic Paleocyanography*. Elsevier, New York, pp. 567–644.
- Caspers, H., 1957. Black Sea and Sea of Azov. J.W. Hedgpeth. *Treatise on marine ecology and paleoecology*: Geological Society of America Memoirs, pp. 801–921.
- Chan, L., Drummond, D., Edmond, J., Grant, B., 1977. On the barium data from the Atlantic GEOSEC Expedition. *Deep-Sea Research* 24, 613–649.
- Codispoti, L.A., Friederich, G.E., Murray, J.W., Sakamoto, C.M., 1991. Chemical variability in the Black Sea: implications of continuous vertical profiles that penetrated the oxic/anoxic interface. *Deep-Sea Research* 38 (2a), 691–710.
- Collier, R.W., 1984. Particulate and dissolved vanadium in the North Pacific Ocean. *Nature (London)* 309, 441–444.
- Collier, R.W., 1985. Molybdenum in the Northeast Pacific Ocean. *Limnology and Oceanography* 30 (6), 1351–1354.
- Collier, R., Edmond, J., 1984. Trace element geochemistry of marine biogenic particulate matter. *Progress in Oceanography* 13, 113–199.
- Crusius, J., Calvert, S., Pedersen, T., Sage, D., 1996. Rhenium and molybdenum enrichments in sediments as indicators of oxic, suboxic and sulfidic conditions of deposition. *Earth and Planetary Science Letters* 145, 65–78.
- Cullen, J.T., Lane, T.W., Morel, F.M.M., Sherrell, R., 1999. Modulation of cadmium uptake in phytoplankton by seawater CO<sub>2</sub> concentration. *Nature* 402 (6758), 165–167.
- Cullen, J.T., Field, M.P., Sherrell, R.M., 2001. The determination of trace elements in filtered suspended marine particulate material by sector field HR-ICP-MS. *Journal of Analytical Atomic Spectrometry* 16, 1307–1312.
- Degens, E.T., Ross, D.A. (Eds.), 1974. *The Black Sea-Geology, chemistry, and biology*. : Memoirs of the American Association of Petroleum Geologists, vol. 20. American Association of Petroleum Geologists, Tulsa, Oklahoma, USA, p. 633.
- Donat, J.R., Bruland, K.W., 1994. Chapter 11: trace elements in the oceans. In: Salbu, S.A. (Ed.), *Trace Elements in Natural Waters*. CRC press, INC., pp. 247–280.
- Dymond, J., Suess, E., Lyle, M., 1992. Barium in deep-sea sediment: a geochemical proxy for paleoproductivity. *Paleoceanography* 7 (2), 163–181.
- Emerson, S., Huested, S., 1991. Ocean anoxia and the concentrations of molybdenum and vanadium in seawater. *Marine Chemistry* 34, 177–196.
- Emerson, S., Jacobs, L., Tebo, B., 1983. The behavior of trace metals in marine anoxic waters: solubilities at the oxygen–hydrogen sulfide interface. In: Wong, C.S., Boyle, E., Bruland, K.W., Burton, J.D., Goldberg, E.D. (Eds.), *Trace Metals in Sea Water*. Plenum Press, New York, pp. 579–608.
- Falkner, K.K., Klinkhammer, G.P., Bowers, T.S., Todd, J.F., Lewis, B.L., Landing, W.M., Edmond, J.M., 1993. The behavior of barium in anoxic marine waters. *Geochimica et Cosmochimica Acta* 57, 537–554.
- Falkner, K.K., Klinkhammer, G.P., Ungerer, A., Christie, D., 1995. Inductively coupled plasma mass spectrometry in geochemistry. *Annual Review of Earth and Planetary Sciences* 23, 409–449.
- Fraustu da Silva, J.J.R., Williams, R.J.P., 1991. *The Biological Chemistry of the Elements*. Clarendon Press, Oxford.
- Fuchsman, C.A., Murray, J.W., Kononov, S.K., 2008. Concentration and natural stable isotope profiles of nitrogen species in the Black Sea. *Marine Chemistry* 111, 90–105.
- Gobeil, C., Macdonald, R.W., Sundby, B., 1997. Diagenetic separation of cadmium and manganese in suboxic continental margin sediments. *Geochimica et Cosmochimica Acta* 61, 4647–4654.
- Guieu, C., Martin, J.M., 2002. Level and fate of metals in the Danube delta plume. *Estuarine, Coastal and Shelf Science* 54 (3), 501–512.
- Haraldsson, C., Westerlund, S., 1988. Trace metals in the water columns of the Black Sea and Framvaren Fjord. *Marine Chemistry* 23, 417–424.
- Haraldsson, C., Westerlund, S., 1991. Total and suspended cadmium, cobalt, copper, iron, lead, manganese, nickel and zinc in the water column of the Black Sea. In: Izdar, E., Murray, J.W. (Eds.), *Black Sea Oceanography: NATO ASI Series*, vol. 351, pp. 161–172.
- Helz, G.R., Miller, C.V., Charnock, J.M., Mosselman, J.F.W., Patrick, R.A.D., Garner, C.G., Vaughan, D.J., 1996. Mechanism of molybdenum removal from the sea and its concentration in black shales: EXFAS evidence. *Geochimica et Cosmochimica Acta* 60, 3631–3642.
- Ho, T.-Y., Quigg, A., Finkel, Z.V., Milligan, A.J., Wyman, K., Falkowski, P.G., Morel, F.M.M., 2003. The elemental composition of some marine phytoplankton. *Journal of Phycology* 39, 1145–1159.
- Ho, T.Y., Wen, L.S., You, C.F., Lee, D.C., 2007. The trace-metal composition of size-fractionated plankton in the South China Sea: biotic versus abiotic sources. *Limnology and Oceanography* 52 (5), 1776–1788.
- Jacobs, L., Emerson, S., 1982. Trace metal solubility in an anoxic fjord. *Earth and Planetary Sciences* 60, 237–252.
- Jacobs, L., Emerson, S., Skei, J., 1985. Partitioning and transport of metals across the O<sub>2</sub>/H<sub>2</sub>S interface in a permanently anoxic basin: Framvaren Fjord, Norway. *Geochimica et Cosmochimica Acta* 49, 1433–1444.
- Jacobs, L., Emerson, S., Huested, S.S., 1987. Trace metal geochemistry in the Cariaco Trench. *Deep-Sea Research* 34, 965–981.
- Klinkhammer, G., Bender, M., 1980. The distribution of manganese in the Pacific Ocean. *Earth and Planetary Science Letters* 46, 361–384.
- Kononov, S.K., Murray, J.W., 2001. Variations in the chemistry of the Black Sea on a time scale of decades (1960–1995). *Journal of Marine Systems* 31, 217–243.
- Kononov, S., Luther III, G.W., Friederich, G.E., Nuzzio, D.B., Tebo, B.M., Murray, J.W., Oguz, T., Glazer, B., Trouwborst, R.E., Clement, R.E., Murray, K.J., Romanov, A.S., 2003. Lateral injection of oxygen with the Bosphorus plume-fingers of oxidizing potential in the Black Sea. *Limnology and Oceanography* 48 (6), 2369–2376.
- Kononov, S., Luther III, G.W., Yucel, M., 2007. Porewater redox species and processes in the Black Sea sediments. *Chemical Geology* 245, 254–274.
- Kramer, D., Cullen, J.T., Christian, J.R., Johnson, W.K., Pedersen, T.F., 2011. Silver in the subarctic northeast Pacific Ocean: explaining the basin scale distribution of silver. *Marine Chemistry* 123 (1–4), 133–142.
- Kryc, K.A., Murray, R.W., Murray, D.W., 2003. Al-to-oxide and Ti-to-organic linkages in biogenic sediment: relationships to paleoexport production and bulk Al/Ti. *Earth and Planetary Science Letters* 211, 125–141.
- Kuss, J., Kremling, K., 1999. Particulate trace element fluxes in the deep northeast Atlantic Ocean. *Deep-Sea Research Part 1* 46 (1), 149–169.
- Langmuir, D., 1978. Uranium solution-mineral equilibria at low temperatures with applications to sedimentary ore deposits. *Geochimica et Cosmochimica Acta* 42, 547–569.
- Lewis, B.L., Landing, W.M., 1991. The biogeochemistry of manganese and iron in the Black Sea. *Deep-Sea Research* 38 (1–2), 773–804.
- Lewis, B.L., Landing, W.M., 1992. The investigation of dissolved and suspended particulate trace metal fractionation in the Black Sea. *Marine Chemistry* 40 (1–2), 105–141.
- Literathy, P., Laszlo, F., 1999. Micropollutants in the Danube River basin. *Water Science and Technology* 40 (10), 17–26.
- Mandernack, K.W., Post, J., Tebo, B.M., 1995. Manganese mineral formation by bacterial spores of a marine *Bacillus*, strain SG-1: evidence for the direct oxidation of Mn(II) to Mn(IV). *Geochimica et Cosmochimica Acta* 59, 4393–4408.
- Martin, J., Knauer, G., 1973. The elemental composition of plankton. *Geochimica et Cosmochimica Acta* 37, 1639–1653.
- Martin, J.H., Bruland, K.W., Broenkow, W.W., 1976. Cadmium transport in the California current. In: Windom, H.L., Duce, R.A. (Eds.), *Marine Pollutant Transfer*. Lexington Books, Heath, Boston, pp. 159–184.
- Martin, J.H., Knauer, G.A., Gordon, R.M., 1983. Silver distributions and fluxes in north-east Pacific waters. *Nature* 305, 306–309.
- McKay, J.L., Pedersen, T.F., 2008. The accumulation of silver in marine sediments: a link to biogenic Ba and marine productivity. *Global Biogeochemical Cycles* 22, GB4010 17 PP.
- Millero, F.J., 1991. The oxidation of H<sub>2</sub>S in the Chesapeake Bay. *Estuarine Coastal and Shelf Science* 33, 521–527.
- Morford, J., Emerson, S., 1999. The geochemistry of redox sensitive trace metals in sediments. *Geochimica et Cosmochimica Acta* 63, 1735–1750.
- Muller, F.L.L., Gulin, S.B., Kalvøy, A., 2001. Chemical speciation of copper and zinc in surface waters of the western Black Sea. *Marine Chemistry* 76 (4), 233–251.
- Muramoto, J., Honjo, S., Fry, B., Hay, B., Howarth, R., 1991. Sulfur, iron and organic carbon fluxes in the Black Sea: sulfur isotopic evidence for origin of sulfur fluxes. *Deep-Sea Research* 38 (2A), 1151–1187.
- Murphy, J., Riley, J.P., 1962. A modified single solution method for the determination of phosphate in natural waters. *Analytical Chimica Acta* 27, 31–36.
- Murray, J., 1974. The surface chemistry of hydrous manganese dioxide. *Journal of Colloidal Interface Science* 46, 357–371.
- Murray, J.W., 1975a. The interaction of metal ions at the manganese dioxide–solution interface. *Geochimica et Cosmochimica Acta* 39 (4), 505–519.

- Murray, J.W., 1975b. The interaction of cobalt with hydrous manganese dioxide. *Geochimica et Cosmochimica Acta* 39 (5), 635–647.
- Murray, J.W., 1979. Iron oxides. In: Burns, R.G. (Ed.), *Marine Minerals: Short Course Notes: Mineralogical Society of America*, vol. 6, pp. 47–98.
- Murray, J.W., Brewer, P.G., 1977. The mechanisms of removal of iron, manganese and other trace metals from seawater. In: Glasby, G.P. (Ed.), *Marine Manganese Deposits*. Elsevier, Holland, pp. 291–325.
- Murray, J.W., Dillard, J.G., 1979. The oxidation of cobalt(II) adsorbed on manganese dioxide. *Geochimica et Cosmochimica Acta* 43, 781–787.
- Murray, R.W., Leinen, M., 1993. Chemical transport to the seafloor of the equatorial Pacific Ocean across a latitudinal transect at 135°W: tracking sedimentary major, minor, trace, and rare earth element fluxes at the Equator and the Intertropical Convergence Zone. *Geochimica et Cosmochimica Acta* 57, 4141–4163.
- Murray, J.W., Yakushev, E., 2006. The suboxic zone in the Black Sea. In: Neretin, L. (Ed.), *Past and Present Water Column Anoxia*. NATO ARW.
- Murray, J.W., Spell, B., Paul, B., 1983. The contrasting geochemistry of manganese and chromium in the eastern tropical Pacific Ocean. In: Wong, C.S., et al. (Ed.), *Trace Metals in Seawater*. Plenum Press, pp. 643–669.
- Murray, J.W., Dillard, J.G., Giovanoli, R., Moers, H., Stumm, W., 1985. Oxidation of Mn (II): initial mineralogy, oxidation state and ageing. *Geochimica et Cosmochimica Acta* 49, 463–470.
- Murray, J.W., Jannasch, H.W., Hojo, S., Anderson, R.F., Reeburgh, W.S., Top, Z., Friederich, G.E., Codispoti, L.A., Izdar, E., 1989. Unexpected changes in the oxic/anoxic interface in the Black Sea. *Nature* 338 (6214), 411–413.
- Murray, J.W., Codispoti, L.A., Friederich, G.E., 1995. Oxidation-reduction environments: the suboxic zone in the Black Sea. In: Huang, C.P., Melia, C.O., Morgan, J.J. (Eds.), *Aquatic Chemistry*. American Chemical Society, pp. 157–176.
- Nameroff, T.J., 1996. The geochemistry of redox-sensitive metals in sediments of the oxygen minimum off Mexico. Ph.D. Thesis, University of Washington, Seattle, WA.
- Nameroff, T.J., Ballistreri, L.S., Murray, J.W., 2002. Suboxic trace metal geochemistry in the eastern tropical north Pacific. *Geochimica et Cosmochimica Acta* 66, 1139–1158.
- Nameroff, T.J., Calvert, S.E., Murray, J.W., 2004. Glacial–interglacial variability in the eastern tropical North Pacific oxygen minimum zone recorded by redox-sensitive trace metals. *Paleoceanography* 19, A1010.
- Oğuz, T., 2002. Role of physical processes controlling oxycline and suboxic layer structures in the Black Sea. *The Black Sea in Crisis: The Need for Concerted International Action 1992: Ambio*, vol. 21 (2).
- Oğuz, T., Murray, J.W., Callahan, A., 2001a. Modeling redox cycling across the suboxic–anoxic interface zone in the Black Sea. *Deep-Sea Research, Part I* 48, 761–787.
- Oğuz, T., Ducklow, H.W., Purcell, J.E., Malanotte-Rizzoli, P., 2001b. Modeling the response of top–down control exerted by gelatinous carnivores on the Black Sea pelagic food web. *Journal of Geophysical Research* 106, 4543–4564.
- Okus, E., Asian-Yilma, A., Yuksek, A., Tas, S., Tufekci, V., 2002. Nutrient distribution in the Bosphorus and surrounding areas. *Water Science and Technology* 46, 59–66.
- Orians, K.J., Boyle, E.A., Bruland, K.W., 1990. Dissolved titanium in the open ocean. *Nature* 348, 322–325.
- Paytan, A., Kastner, M., 1996. Benthic Ba fluxes in the central equatorial Pacific, implications for the oceanic Ba cycle. *Earth and Planetary Science Letters* 142, 439–450.
- Paytan, A., Kastner, M., Chavez, F., 1996. Glacial to interglacial fluctuations in productivity in the equatorial Pacific as indicated by marine barite. *Science* 274, 1355–1357.
- Piper, D.Z., Calvert, S.E., 2009. A marine biogeochemical perspective on black shale deposition. *Earth-Science Reviews* 95 (1–2), 63–96.
- Piper, D.Z., Calvert, S.E., in press. Holocene and late glacial Paleoceneanography and Paleolimnology of the Black Sea: Changing sediment provenance and basin hydrography over the past 20,000 years. *Geochimica et Cosmochimica Acta*.
- Raven, J.A., 1988. The iron and molybdenum use efficiencies of plant growth with different energy, carbon and nitrogen sources. *New Phytologist* 109, 279–287.
- Ricking, M., Tertyze, K., 1999. Trace metals and organic compounds in sediment samples from the River Danube in Russe and Lake Srebarna (Bulgaria). *Environmental Geology* 37 (1–2), 40–46.
- Rue, E.L., Smith, G.J., Cutter, G.A., Bruland, K.W., 1997. The response of trace element redox couples to suboxic conditions in the water column. *Deep-Sea Research* 44, 113–134.
- Saager, P.M., De Baar, H.J.W., Howland, R.J., 1992. Cd, Zn, Ni, and Cu in the Indian Ocean. *Deep-Sea Research* 39, 9–35.
- Sañudo-Wilhelmy, S.A., Flegal, A.R., 1992. Anthropogenic silver in the Southern California Bight: a new tracer of sewage in coastal waters. *Environmental Science and Technology* 26, 2147–2151.
- Saydam, C., Tugrul, S., Basturk, O., Oğuz, T., 1993. Identification of the oxic/anoxic interface surfaces in the Black Sea. *Deep-Sea Research I* 40 (7), 1405–1412.
- Shaffer, G., 1986. Phosphate pumps and shuttles in the Black Sea. *Nature* 321, 515–517.
- Skrabal, S.A., 2006. Dissolved titanium distributions in the Mid-Atlantic Bight. *Marine Chemistry* 102, 218–229.
- Skrabal, S.A., Terry, C.M., 2002. Distributions of dissolved titanium in porewaters of estuarine and coastal marine sediments. *Marine Chemistry* 77, 109–122.
- Sorokin, Y.I., 1983. The Black Sea. In: Ketchum, B.H. (Ed.), *Ecosystems of the World 26: Estuaries and Enclosed Seas*. Elsevier, Amsterdam, pp. 253–292.
- Spencer, D.W., Brewer, P.G., 1971. Vertical advection, diffusion and redox potentials as controls on the distribution of manganese and other trace metals dissolved in waters of the Black Sea. *Journal of Geophysical Research* 76, 5877–5892.
- Spencer, D.W., Brewer, P.G., Sachs, P.L., Smith, C.L., 1971. The distribution of some chemical elements between dissolved and particulate phases in the ocean. *AEC Rep. NYO-4150-2*. 41 pp.
- Spencer, D.W., Brewer, P.G., Sachs, P.L., 1972. Aspects of the distribution and trace element composition of suspended matter in the Black Sea. *Geochimica et Cosmochimica Acta* 36 (1), 71–86.
- Stiefel, E.I., 1996. Molybdenum bolsters the bioinorganic brigade. *Science* 272 (5268), 1599–1600.
- Stumm, W., Morgan, J.J., 1981. *Aquatic Chemistry: An Introduction Emphasizing Chemical Equilibria in Natural Waters*. John Wiley and Sons, New York, NY, p. 780.
- Stumm, W., Morgan, J.J., 1996. *Aquatic Chemistry*, 3rd edition. John Wiley and Sons, New York.
- Suess, E., 1979. Mineral phases formed in anoxic sediments by microbial decomposition of organic matter. *Geochimica et Cosmochimica Acta* 43, 339–352.
- Tankere, S.P.C., Muller, F.L.L., Burton, J.D., Statham, P.J., Guieu, C., Martin, J.M., 2001. Trace metal distributions in shelf waters of the northwestern Black Sea. *Continental Shelf Research* 21, 1501–1532.
- Taylor, S.R., 1964. Abundance of chemical elements in the continental crust: a new table. *Geochimica et Cosmochimica Acta* 28, 1273–1285.
- Taylor, S.R., McLennan, S.M., 1985. *The Continental Crust: Its Composition and Evolution*. Blackwell, Oxford, p. 312.
- Taylor, S.R., McLennan, S.M., 1995. The geochemical evolution of the continental crust. *Reviews in Geophysics* 33, 241–265.
- Tebo, B.M., 1991. Manganese (II) oxidation in the suboxic zone of the Black Sea. *Deep-Sea Research* 38 (2), 883–905.
- Tebo, B.M., Bargar, J.R., Clement, B.G., Dick, G.J., Murray, K.J., Parker, D., Verity, R., Webb, S.M., 2004. Biogenic manganese oxides: properties and mechanisms of formation. *Annual Reviews of Earth and Planetary Science* 32, 287–328.
- Trouwborst, R.E., Clement, B.G., Tebo, B.M., Glazer, B.T., Luther III, G.W., 2006. Soluble (Mn(III) in suboxic zones. *Science* 313, 1955–1957.
- Tuğrul, S., Bastürk, O., Saydam, C., Yilmaz, A., 1992. Changes in the hydrochemistry of the Black Sea inferred from density profiles. *Nature* 359, 137–139.
- Twining, B.S., Baines, S.B., Fisher, N.S., 2004. Element stoichiometries of individual plankton cells collected during the Southern Ocean Iron Experiment (SOFeX). *Limnology and Oceanography* 49, 2115–2128.
- Twining, B.S., Nuñez-Milland, D., Vogt, S., Johnson, R.S., Sedwick, P.N., 2010. Variations in *Synechococcus* cell quotas of phosphorus, sulfur, manganese, iron, nickel, and zinc within mesoscale eddies in the Sargasso Sea. *Limnology and Oceanography* 55 (2), 492–506.
- Twining, B.S., Baines, S.B., Bozard, J.B., Vogt, S., Walker, E.A., Nelson, D.M., 2011. Metal quotas of plankton in the equatorial Pacific Ocean. *Deep-Sea Research II* 58, 325–341.
- Vinogradov, M.Y., Nalbandov, Y.R., 1990. Effect of changes in water density on the profiles of physicochemical and biological characteristics in the pelagic ecosystem of the Black Sea. *Oceanology* 30, 567–573.
- Wanty, R.B., Goldhaber, M.B., 1992. Thermodynamics and kinetics of reactions involving vanadium in natural systems: accumulation of vanadium in sedimentary rocks. *Geochimica et Cosmochimica Acta* 56, 1471–1484.
- Wanty, R.B., Goldhaber, M.B., Northrop, H.R., 1990. Geochemistry of vanadium in an epigenetic sandstone-hosted vanadium–uranium deposit, Henry basin, Utah. *Economic Geology* 85, 270–284.
- Wedepohl, K.H., 1968. *Origin and Distribution of the Elements*. Pergamon Press, London.
- Wedepohl, K.H., 1995. The composition of the continental crust. *Geochimica et Cosmochimica Acta* 59 (7), 1217–1232.
- Wehrli, B., Stumm, W., 1989. Vanadyl in natural waters: adsorption and hydrolysis promote oxygenation. *Geochimica et Cosmochimica Acta* 53, 69–77.
- Wei, C.L., Murray, J.W., 1994. The behavior of scavenging isotopes in marine anoxic environments: lead -210 and polonium -210 in the water column of the Black Sea. *Geochimica et Cosmochimica Acta* 58, 1795–1812.
- Yarincik, K., Murray, R., Peterson, L., 2000. Climatically sensitive eolian and hemipelagic deposition in the Cariaco Basin, Venezuela, over the past 580,000 years: results from Al/Ti and K/Al. *Paleoceanography* 15, 210–228.
- Yemenicioğlu, S., Erdogan, S., Tugrul, S., 2006. Distribution of dissolved forms of iron and manganese in the Black Sea. *Deep-Sea Research Part II: Topical Studies in Oceanography* 53 (17–19), 1842–1855.
- Yiğiterhan, O., 2005. Trace metal composition of particulate matter in the water column and sediments of the Black Sea and regional rivers. PhD Thesis, Middle East Technical University, pp. 324.
- Yiğiterhan, O., Murray, J.W., 2008. Trace metal composition of particulate matter of the Danube River and Turkish rivers draining into the Black Sea. *Marine Chemistry* 111, 63–76.
- Yiğiterhan, O., Murray, J.W., Tuğrul, S., Yemenicioğlu, S., (in preparation). Change of particles composition in the Black Sea from river input to ultimate burial. (In: *Marine Chemistry* (format)).
- Zheng, Y., Anderson, R.F., van Geen, A., Kuwabara, J., 2000. Authigenic molybdenum formation in marine sediments: a link to porewater sulfide in the Santa Barbara Basin. *Geochimica et Cosmochimica Acta*. 64, 4165–4178.